Chronostratigraphy of the Barremian-Early Albian of the Maestrat Basin (E Iberian Peninsula): integrating strontium-isotope stratigraphy and ammonoid biostratigraphy

Telm Bover-Arnal [a,*], Josep A. Moreno-Bedmar [b], Gianluca Frijia [c], Enric Pascual-Cebrian [d], Ramon Salas [a]

[a] *Departament de Geoquímica, Petrologia i Prospecció Geològica, Facultat de Geologia, Universitat de Barcelona, Martí i Franquès s/n, 08028 Barcelona, Spain*
[b] *Instituto de Geología, Universidad Nacional Autónoma de México, Ciudad Universitaria, Coyoacán, 04510 México D.F., Mexico*
[c] *Institut für Erd- und Umweltwissenschaften, Universität Potsdam, Karl Liebknecht-Str. 24-25, Potsdam-Golm 14476, Germany*
[d] *GeoScience Limited, Falmouth Business Park, Bickland Water Road, Falmouth TR11 4SZ, UK*

* Corresponding author.
E-mail address: telm.boverarnal@ub.edu (T. Bover-Arnal).

Abstract. A revised chronostratigraphy of the Barremian-Early Albian sedimentary record of the Maestrat Basin (E Iberian Peninsula) is provided based on a comprehensive synthesis of previous biostratigrahic data, a new ammonoid finding and numerical ages derived from $^{87}Sr/^{86}Sr$ values measured on shells of rudists, oysters and brachiopods. The succession, which comprises eight lithostratigraphic formations, is arranged into six major transgressive-regressive sequences and plotted against numerical ages, geomagnetic polarity chrons, ammonoid zones and the stratigraphic distribution of age-diagnostic ammonoids, orbitolinid foraminifera and rudist bivalves. The oldest lithostratigraphic unit sampled, the marine Artoles Formation, is Early to Late Barremian. Above, the dinosaur-bearing deposits of the Morella Formation and its coastal to shallow-marine equivalent, the Cervera del Maestrat Formation, are of Late Barremian age and span at least part of the *Imerites giraudi* ammonoid zone. $^{87}Sr/^{86}Sr$ ratios from oyster shells in the upper part of the overlying marine Xert Formation are consistent with a latest Barremian-earliest Aptian age, while an ammonite belonging to the Late Barremian *Martelites sarasini* Zone was collected within the lowermost part of this latter formation. The Barremian-Aptian boundary is tentatively placed close above the base of the succeeding transgressive marls of the Forcall Formation by analogy with nearby Tethyan basins, where major transgressive records contain latest Barremian ammonoids in their basal parts. The rest of the Forcall Formation and the platform carbonates of the Villarroya de los Pinares Formation are of Early Aptian age. The transition from the Barremian into the Aptian occurred in the course of a wide transgression, which was accompanied by the proliferation of *Palorbitolina lenticularis*. This transgressive event drowned Late Barremian carbonate platforms (Xert Formation) throughout the basin. Extensive carbonate platforms (Villarroya de los Pinares Formation) recovered coevally with a post-OAE1a late Early Aptian major regression of relative sea level. The last lithostratigraphic unit analyzed, the marine Benassal Formation, spans the terminal Early Aptian-Late Aptian interval. Based on ammonite distributions, the lower part of the overlying coastal to continental coal-bearing Escucha Formation is Early Albian in age. This improved chronostratigraphic knowledge allows a more precise correlation of the sedimentary record studied with other coeval successions worldwide.

Key words. Strontium-isotope stratigraphy, Geochronology, Biostratigraphy, Ammonoids, Early Cretaceous, Iberian Chain, Tethys

1. Introduction

In the Maestrat Basin (Fig. 1), the boundary between the Barremian and the Aptian stages has been classically placed within the Artoles Formation (boundary A1 in Fig. 2; e.g., Salas 1987, Salas et al. 1995, 2001, Aurell and Vennin 2001, Liesa et al. 2006, Embry et al. 2010) or at the limit between the Artoles and the Morella/Cervera del Maestrat formations (boundary A2 in Fig. 2; e.g., Gàmez et al. 2003, Salas et al. 2005, Moreno-Bedmar et al. 2009, 2010, Bover-Arnal et al. 2009, 2010). The stratigraphic calibration of this boundary was mainly based on charophyte, ostracod and/or benthic foraminifera biostratigraphic data (e.g., Canérot et al. 1982, Salas et al. 1995) and geomagnetic polarity (e.g., Salas et al. 2005). However, and besides the above-mentioned chronostratigraphic discrepancy between studies, Canérot et al. (1982) and López Llorens (2007) already noted that the stratigraphic position of the Barremian-Aptian boundary in the Maestrat Basin was not successfully established yet. Thus, while depicting the Barremian/Aptian boundary at the limit between the Morella (or Cervera del Maestrat) and Xert formations, Canerot et al. (1982, Fig. 6.1, p. 277), in their descriptions of lithostratigraphic units, by contrast, give a terminal Barremian or earliest Aptian age for the Morella Formation (p. 285) and a terminal Barremian to earliest Aptian time span for its coastal to marine equivalent the Cervera del Maestrat Formation (p. 284). On the other hand, López Llorens (2007) found an *Argvethites* sp. (genus determination modified in Garcia et al. 2014), a Late Barremian ammonite belonging to the *Imerites giraudi* Zone, within the marine-influenced deposits of the uppermost part of the Morella Formation, thus ruling out the Early Aptian age classically assumed for this lithostratigraphic unit.

Later on, Moreno-Bedmar and Garcia (2011) put forward the hypothesis that the Barremian-Aptian boundary was located at the lowermost part of the marls of the Forcall Formation (boundary B in Fig. 2). This supposition was founded on the recognition of the *Deshayesites oglanlensis* ammonoid Zone and the Subzone *Deshayesites luppovi* at the lower part of the marls of the Forcall Formation. Moreno-Bedmar and Garcia (2011) also noted that the Organyà Basin in north-eastern Spain and the Provençal Platform in south-eastern France recorded a major transgressive event starting in the latest Barremian that would then be analogous to the deposition of the hemipelagic marls of the Forcall Formation in the Maestrat Basin (E Spain). Since then, Garcia et al. (2014) and Villanueva-Amadoz et al. (2014) have attempted to test this hypothesis by reviewing the literature and providing new data on the Barremian-Aptian ammonite biostratigraphy of the Maestrat Basin and by studying the palynological content of the Morella Formation. Even though neither of these two works is conclusive, they lend support to the Moreno-Bedmar and Garcia (2011) hypothesis. Garcia et al. (2014) identified the species *Deshayesites antiquus* Bogdanova and *Deshayesites* sp. cf. *oglanlensis* Bogdanova in the lower, non-basal part of the marls of the Forcall Formation. These species are characteristic of the lower part of the *Deshayesites oglanlensis* Zone, which is the first Aptian ammonoid Zone (Fig. 3; Reboulet et al. 2011, 2014). Villanueva-Amadoz et al. (2014) record the dinoflagellate cysts *Subtilisphaera terrula*, *Florentinia mantelli* and *Oligosphaeridium abaculum*, which indicate a Barremian age, from the base of the Morella Formation. Villanueva-Amadoz et al. (2014) also recognize the pollen type *Stellatopollis* sp. in the upper part of the Morella Formation and indicate that possibly this formation may be as old as Late Barremian.

Using strontium-isotope stratigraphy and new ammonite biostratigraphic data the present study conclusively locates the Barremian-Aptian boundary, while also calibrating the age of the Barremian-Early Albian lithostratigraphic units of the Maestrat Basin. Strontium-isotope stratigraphy is today a well-established, proven and widely adopted chemostratigraphic method, which allows derivation of numerical ages from known past changes in the $^{87}Sr/^{86}Sr$ ratio of seawater (e.g., Steuber 1999, 2001, 2003a, b, McArthur et al. 2001, 2012, McArthur and Howarth 2004, Steuber et al. 2005, Frijia and Parente 2008, Bodin et al. 2009, Burla et al. 2009, Boix et al. 2011, Huck et al. 2011, Steuber and Schlüter 2012, Wagreich et al. 2012, Williamson et al. 2012, Jaramillo-Vogel et al. 2013, Bonilla-Rodríguez et al. 2014, Pascual-Cebrian 2014, Frijia et al. 2015). The resulting numerical ages derived from $^{87}Sr/^{86}Sr$ values obtained from brachiopod, rudist and oyster shells collected in selected stratigraphic intervals of the Barremian-Early Albian sedimentary succession of the Maestrat

Basin are plotted against lithostratigraphic units, major transgressive-regressive sequences of relative sea level recorded in the basin, ammonoid zones, geomagnetic polarity chrons, and ammonite, orbitolinid and rudist occurrences (Fig. 3). The results are complemented with numerical ages derived from $^{87}Sr/^{86}Sr$ ratios measured in rudist shells from the western Maestrat Basin by Pascual-Cebrian (2014).

Therefore, besides constraining the stratigraphic position of the Barremian-Aptian boundary in the Maestrat Basin, the resulting chronostratigraphic framework (Fig. 3) allows us: i) to establish the age of the dinosaur and other vertebrate records found in the Morella and Xert formations (e.g., Yagüe et al. 2003, Canudo et al. 2008a, b, Jorquera-Grau et al. 2009, Pérez-García et al. 2009, 2014, Gasulla et al. 2011a, 2011b, 2012); ii) to date the major Barremian-Early Albian transgressive-regressive trends of relative sea level and the episodes of carbonate platform development, subaerial exposure and drowning in the basin; iii) to give a more precise correlation of the sedimentary record studied with other coeval successions worldwide, and iv) to test the numerical-age calibrations of Tethyan Barremian-Early Albian ammonoid, orbitolinid and rudist species ranges and the biostratigraphic correlation between their different zonations.

--------------------------------- Figure 1 (width of page) near here --------------------------------

2. Geological setting

The Maestrat Basin was an intracratonic Mesozoic rift basin located at the eastern margin of the Iberian plate that developed on account of tectonic extension linked to the opening and spreading of the Neotethys towards the west, and the opening of the Central Atlantic Ocean and the Bay of Biscay (Salas and Casas 1993). From the Tithonian (Late

Jurassic) to the Albian (Early Cretaceous), the Maestrat Basin was structured into seven sub-basins: Aliaga, El Perelló, Galve, Morella, Oliete, Penyagolosa and Salzedella (Salas and Guimerà 1996; Fig. 1B). Throughout the Barremian-Early Albian time interval reviewed in this paper, up to 2 km-thick continental to hemipelagic mixed carbonate-siliciclastic sedimentary successions were deposited within these sub-basins (Canérot et al. 1982; Salas 1987). Later on, during the Paleogene-Early Miocene, and due to the collision between the Iberian and European plates in the course of the Alpine orogeny, the Maestrat Basin was inverted and gave rise to the eastern part of the Iberian Chain (E Iberian Peninsula; Fig. 1A) (Salas et al. 2001).

--------------------------------- Figure 2 (width of column) near here --------------------------------

2.1. Barremian-Early Albian lithostratigraphy

The Barremian-Early Albian sedimentary record from the Maestrat Basin can be subdivided into eight lithostratigraphic units with the rank of formations. These formations are named from oldest to youngest as Artoles, Cervera del Maestrat, Morella, Xert, Forcall, Villarroya de los Pinares, Benassal and Escucha (Fig. 3; Canérot et al. 1982, Salas 1987, Salas et al. 1995, 2001).

The marine Artoles Formation (Figs 3 and 5A) is mainly characterized by an alternation of marls, sandy limestones and limestones rich in oysters (Salas 1987, Salas et al. 1995, 2001, Caja 2004). Above, fluviatile red clays and sandstones associated with vertebrate fossils constitute the Morella Formation (Figs 3 and 5A-B; Canérot et al. 1982, Salas 1987, Salas et al. 1995, Gàmez et al. 2003). Bioclastic and sandy limestones in the upper part of the Morella Formation indicate punctuated episodes of coastal to marine influence (Figs 3 and

5A-B; Canérot et al. 1982). The Morella Formation passes laterally to the mixed carbonate-siliciclastic coastal to shallow-marine deposits of the Cervera del Maestrat Formation (Figs 3, 5C and 6A; Canérot et al. 1982, Salas 1987, Salas et al. 1995). The overlying Xert Formation (Figs 3, 5A, 6 and 7A) consists of an alternation of marine sandstones, sandy limestones and marls, which evolve into massive limestones containing abundant orbitolinids in the upper part of the formation (Canérot et al. 1982, Salas 1987, Salas et al. 1995, Vennin and Aurell 2001, Bover-Arnal et al. 2010, Embry et al. 2010).

The Forcall Formation (Figs 3, 6 and 7A-C) is mainly made up of basin marls with interbedded marly limestones, silty limestones, sandy limestones and limestones characterized by fossil biota such as ammonoids and *Palorbitolina lenticularis* (Canérot et al. 1982, Salas 1987, Salas et al. 1995, Clariana 1999, Moreno-Bedmar et al. 2010a). The four Early Aptian ammonoid zones namely, *Deshayesites oglanlensis*, *Deshayesites forbesi*, *Deshayesites deshayesi* and *Dufrenoyia furcata*, are recorded within this formation (Fig. 3; Moreno-Bedmar et al. 2010a, Garcia et al. 2014). The C-isotope shifts linked to the Early Aptian oceanic anoxic event (OAE1a) have been located at the upper part of the *Deshayesites forbesi* Zone within the Forcall Formation (Fig. 3; Moreno-Bedmar et al. 2009a, Bover-Arnal et al. 2010, 2011b, Cors et al. 2015). The position of the OAE1a within the *Deshayesites forbesi* Zone (and not within the *Deshayesites deshayesi* Zone as often reported by other workers, notably in the Vocontian Basin in France, e.g., Moullade et al. 2015) is not related to any dischronism of the OAE1a or to a later first appearance datum of *Deshayesites deshayesi* in the Maestrat Basin, but rather to a disagreement between authors about the taxonomic identification of *Deshayesites deshayesi* (see Moreno-Bedmar et al. 2009, 2014).

The succeeding lithostratigraphic unit, the Villarroya de los Pinares Formation (Figs 3, 6 and 7A, C; Canérot et al. 1982, Salas 1987, Salas et al. 1995, Clariana 1999, Clariana et al. 2000), is characterized by sandy limestones, oolitic, peloidal and skeletal packstones and grainstones, and platform carbonates with floatstone to rudstone textures containing rudist bivalves and corals. Locally, the Villarroya de los Pinares Formation is also constituted by mudstones with ammonites, planktic foraminifera and sponge spicules. The Villarroya de los Pinares Formation passes basinwards to the marls of the Forcall Formation (Fig. 3; see Bover-Arnal et al. 2009).

The Benassal Formation consists of an alternation of marly intervals containing bivalves, gastropods and locally, scleractinian corals, and platform carbonates dominated by rudist bivalves, colonial corals and nerineid gastropods (Figs 3, 6A, 7A, C-D and 8A-B; Salas 1987, Tomás et al. 2008, Bover-Arnal et al. 2010, Martín-Martín et al. 2013, 2015, Gomez-Rivas et al. 2014). The uppermost part of the Benassal Formation is formed by ferruginous ooid grainstones, sandstones, sandy limestones and clays indicating a progressive shallowing of the depositional environment (Figs 3, 6A and 8B; Canérot et al. 1982, Salas 1987, Bover-Arnal et al. 2010). This formation registered the uppermost part of the *Dufrenoyia furcata* Zone at its base (Fig. 3; Moreno-Bedmar et al. 2012, Bover-Arnal et al. 2014, Garcia et al. 2014). Ammonoid specimens belonging to the *Epicheloniceras martini*, *Parahoplites melchioris* and *Acanthoplites nolani* zones have been found along the Benassal Formation (Fig. 3; Weisser 1959, Moreno-Bedmar et al. 2010a, Martín-Martín et al. 2013, Garcia et al. 2014).

Above, the Escucha Formation mainly corresponds to an alternation of clays, coal levels and sandstones (Figs 3 and 8C; Aguilar et al. 1971, Pardo 1979, Pardo and Villena 1979, Canérot et al. 1982, Querol 1990, Querol et al. 1992). Locally, the limit between the Benassal and Escucha formations corresponds to an erosional unconformity (Canérot et al. 1982, Salas 1987, Querol et al. 1992, Salas et al. 1995). In the depocentre of the Maestrat Basin, which is located in the northeastern part of the Salzedella sub-basin (Fig. 1B), the lower part of the Escucha Formation was dated by means of ammonoids as earliest Albian (Fig. 3; Moreno-Bedmar et al. 2008, Garcia et al. 2014).

------------ Figures 3 and 4 (width of page - both figures situated side by side) near here -------------

3. Materials and methods

3.1. Terminology

In this paper, the stratigraphic terminology of time-rock units and geologic time units is unified following Zalasiewicz et al. (2004). Accordingly, the paper uses "early" and "late", but not "lower" and "upper", to define both chronostratigraphical and geochronological terms.

3.2. Lithostratigraphic units and localities sampled

Seven samples for strontium-isotope stratigraphy were collected from three different stratigraphic levels within the Artoles Formation in the Salzedella sub-basin (Fig. 1B). Two brachiopods, pieces A1-A and A1-B (Fig. 3 and Table 1A), and two oyster shells, specimens A2-A and A2-B (Fig. 3 and Table 1A), were sampled in the lower-middle part of this lithostratigraphic unit in the Corral d'en Parra section (UTM coordinates: X=31T 263453, Y=4482816; see Salas 1987), in the outskirts of the town of Sant Mateu (*Comarca* of El Baix Maestrat). In addition, three oyster specimens, A3-A, A3-B and A3-C (Fig. 3 and Table 1A), were taken at the upper part of the Artoles Formation cropping out along the road N-232, in Mas del Regall (UTM coordinates: X=31T 257351, Y=4489393; see Salas 1987), in the surroundings of the town of Xert (*Comarca* of El Baix Maestrat).

Three oyster valves, samples C1-A, C1-B and C1-C (Fig. 3 and Table 1A), were collected in the lower part of the Cervera del Maestrat Formation in the Salzedella sub-basin (Fig. 1B). The sampling locality corresponds to Mas del Regall section (UTM coordinates: X=31T 257612, Y=4489753; see Salas 1987), which crops out 2.2 km to the west of the town of Xert (*Comarca* of El Baix Maestrat).

The two oyster shells, specimens X1-A and X1-B (Fig. 3 and Table 1 A), sampled to calibrate the age of the Xert Formation, come from the Salzedella sub-basin (Fig. 1B). These low-Mg calcite pieces were collected in the upper part of this lithostratigraphic unit exposed along the forest road (UTM coordinates: X=31T 258579, Y=4490741; see Salas 1987) that goes from the town of Xert (*Comarca* of El Baix Maestrat) to the Turmell Range (*Comarca* of Els Ports).

Finally, three rudist shells, samples B1-A, B1-B and B1-C (Fig. 3 and Table 1A), were plucked from the Benassal Formation in the Morella sub-basin (Fig. 1B). The stratigraphic level sampled corresponds to the upper part of transgressive incised valley-fill deposits, which are found at the Mola d'en Camaràs (UTM coordinates: X=30T 740119, Y=4503220.80; see Bover-Arnal et al. 2014), 3 km to the northeast of the town of El Forcall (*Comarca* of Els Ports).

3.3. Strontium-isotope stratigraphy

The analytical and chronostratigraphic data presented in Table 1A were obtained from 15 samples collected for this study. These results were integrated with the dataset of Pascual-Cebrian (2014) (Table 1B) who performed strontium-isotope stratigraphic analyses on 5 rudist shells collected in the Forcall, Villarroya de los Pinares and Benassal formations in the western Maestrat Basin (Galve sub-basin; Fig. 1B). In the present work, the samples studied by Pascual-Cebrian (2014) have been renumbered for simplicity: F1 = LC-Sr-1; V1 = LSC-Sr-3; V2 = LSC-Sr-1; V3 = Mi-Sr-2; B2 = BC-Sr-1 (Fig. 3 and Table 1B). Sample F1 was collected within the *Lithocodium aggregatum*-bearing horizon found in the Forcall Formation cropping out in Las Cubetas section (Fig. 1B; UTM coordinates: X=30T 694192.131, Y=4504314.076; see Bover-Arnal et al. 2010, 2011b for sample locality details). Samples V1 and V2 come from the lower part of the Villarroya de los Pinares Formation in La Serna (Fig. 1B; UTM coordinates: X=30T 693819.913, Y=4490421.394; see Bover-Arnal et al. 2015 for location of samples). Specimen V3 was collected in the upper part of the Villarroya de los Pinares Formation in Las Mingachas locality (Fig. 1B; UTM coordinates: X=30T 693684.184, Y=4494385.624; see Bover-Arnal et al. 2009 for sample locality details). Specimen B2 was sampled in the lower part of the Benassal Formation in the Las Corralizas section (Fig. 1B; UTM coordinates: X=30T 693993.535, Y=4492353.315; see Bover-Arnal et al. 2010 for location of sample). The selection process and preparation of these samples, as well as the methodology followed to obtain the $^{87}Sr/^{86}Sr$ ratios and derived numerical ages, are described in Pascual-Cebrian (2014).

The new analytical data were measured in biotic low Mg-calcite (mainly oysters and a few rudists and brachiopods) coming from 4 different localities (Figs. 1B and 3; Table 1A). Whenever possible, multiple samples were collected from each stratigraphic level, in order to test the internal consistency of the data. Laboratory preparation of the biotic low Mg-calcite for analysis followed the method described in Frijia and Parente (2008) and Boix et al. (2011). Rock samples and larger shells were cut to produce 0.5−2 cm-thick slabs. These were ground and polished on all sides in order to eliminate superficial contamination. Isolated shells and fragments were washed, through repeated cycles, in an ultrasound bath filled with a solution of deionised water and H_2O_2 5% at 50 °C for 5 minutes to remove adhering clay minerals and then dried at room temperature. Furthermore, some shell was treated for 20 to 45 seconds in HCL 1M, to eliminate calcite overgrowths, and then rinsed carefully with deionised water. As a final step all the samples were washed ultrasonically in a bath of ultrapure water (milli-Q water) for 3 minutes and then dried in a clean environment. All the samples (rock slabs and isolated shell fragments) were then passed through a complete petrographic screening (optical microscope and scanning electron microscope) to assess the preservation of the original shell microstructure.

The elemental (Mg, Sr, Mn and Fe) composition of the shells was analysed as a further screening step. The micritic matrix of some samples was also analysed in order to get deeper insight into the diagenetic processes. Samples for geochemical analyses were obtained by microsampling, under the microscope, of selected areas of polished slabs and shell fragments with a hand-operated microdrill equipped with 0.3 to 0.5 mm ∅ tungsten drill bits. Two splits of each sample were prepared. The first split was used for the ICP-AES analysis of Mg, Sr, Fe and Mn concentration. The second split of the powdered samples was used for strontium-isotope analysis. Geochemical analyses were performed at the Institute for Geology, Mineralogy and Geophysics of the Ruhr-University (Bochum, Germany). After strontium separation by standard ion-exchange methods, strontium-isotope ratios were analyzed on a Finnigan MAT 262 thermal-ionisation mass spectrometer and normalized to an $^{86}Sr/^{88}Sr$ value of 0.1194. The mean value of the USGS EN-1 (modern seawater) standards run together with the samples analysed for this study is 0.709174 ± 0.000006 (2 s.e., n= 4). The $^{87}Sr/^{86}Sr$ ratios of the samples were adjusted to a value of 0.709175 for the USGS EN-1 standard, to be consistent with the normalisation used in the compilation of the look-up table of McArthur et al. (2001; version 4: 08/04). A mean value was calculated when more than one sample was available for one stratigraphic level. The precision of the $^{87}Sr/^{86}Sr$ mean value for each stratigraphic level is given as 2 s.e. of the mean when the number of samples (n) is ≥4. When n<4, the precision is considered to be not better than the average precision of single measurements and is calculated from the standard deviation of the mean value of the standards run with the samples (±0.000013 for n=1, ±0.000009 for n=2 and ±0.000007 for n=3).

The numerical ages of the samples analysed in this study were derived from the look-up table of McArthur et al. (2001, version 4: 08/04, see procedure regarding age calculation in Frijia et al. 2015), which is tied to the Geological Time Scale of Gradstein et al. (2004; hereinafter GTS2004). Minimum and maximum ages were obtained by combining the statistical uncertainty (2 s.e.) of the mean values of the Sr-isotope ratios of the samples with the uncertainty of the seawater curve. The numerical ages were then translated into chronostratigraphic ages and corresponding standard ammonite biozones by reference to the GTS2004.

3.4. Transgressive-regressive sequence-stratigraphic model

The transgressive-regressive sequence-stratigraphic framework is based on the recognition of subaerial unconformity surfaces, maximum flooding surfaces, maximum flooding zones, transgressive surfaces, changes in stacking patterns of lithostratigraphic units and the observed facies succession at the scale of formations by Pardo (1979), Pardo and Villena (1990), Salas (1987), Canérot et al. (1982), Querol (1990), Querol et al. (1992), Vennin and Aurell (2001), Bover-Arnal et al. (2009, 2010, 2011b, 2014, 2015), Embry et al. (2010) and Martín-Martín et al. (2013). Previous sequence-stratigraphic analyses carried out in the basin were also taken into account (e.g., Salas 1987, Salas et al. 2001, Vennin and Aurell 2001, Bover-Arnal et al. 2009, 2010, 2011a, 2014, 2015, Embry et al. 2010, Martín-Martín et al. 2013). See Catuneanu et al. (2009, 2011) for the conceptual background of the transgressive-regressive sequence-stratigraphic method.

--------------------------------- Figure 5 (width of page) near here --------------------------------

--------------------------------- Figure 6 (width of page) near here --------------------------------

--------------------------------- Figure 7 (width of page) near here --------------------------------

--------------------------------- Figure 8 (width of page) near here --------------------------------

4. Preservation of the original Sr-isotope signal

The first and most critical step in order to correctly perform strontium-isotope stratigraphy is to evaluate the preservation of the analysed material. Diagenetic processes can alter significatively the original marine $^{87}Sr/^{86}Sr$ signal leading to a wrong age derivation/calculation. The diagenetic screening approach used in this study to assess the preservation of the analysed fossils followed that described in similar previous works (Steuber et al. 2005, Boix et al. 2011, Frijia and Parente 2008, Frijia et al. 2015).

Analysis of the concentration of some major and trace elements is a powerful tool to estimate the degree of alteration of a bioclastic sample. In this respect, a pattern of lower Sr concentrations, and higher Mn and Fe concentrations and $^{87}Sr/^{86}Sr$ ratios has been commonly associated with a significant degree of diagenetic alteration in multicomponent studies in carbonates (Brand and Veizer 1980, Al-Aasm and Veizer 1986, Brand et al. 2012).

However, in the resulting dataset such a diagenetic covariation is not detectable, with shells and matrix (mixture of pristine and diagenetic phases) both showing Fe and Mn concentrations quite variable with respect to Sr (Table 1A). Frijia et al. (2015) pointed out that relatively high Fe and Mn concentrations are not always indicators of diagenetic processes. High Fe and Mn concentrations occur in shells rather due to contamination from surface oxide coatings than due to recrystallization or incorporation. On the other hand, relatively low Fe and Mn concentrations have been found also in diagenetic calcite (Steuber et al. 2005, Frijia and Parente 2008, Boix et al. 2011, Vicedo et al. 2011, Frijia et al. 2015). The micritic matrix samples analyzed exhibit the highest values for these two elements (Fe up to 7812 ppm and Mn up to 492 ppm; Table 1A), suggesting diagenetic fluids rich in Fe and Mn. Therefore, even if we mainly rely on Sr concentration as the prime criterion of diagenetic screening (Sr > 750 ppm as indicated in Frijia et al. 2015), we also use concentrations of Fe < 250 ppm and Mn < 50 ppm as conservative threshold values to help discriminating between samples which have retained their pristine isotopic composition and samples that have incorporated significant amounts of diagenetic Sr (see references in Frijia et al. 2015).

The next step of the diagenetic screening procedure is to compare the Sr concentration and the Sr-isotope value of the different shells and matrix from the same level. The data show that the micritic matrix has lower Sr concentrations and significantly higher Sr-isotope values than pristine shells. This is the trend expected for diagenetic alteration or for mixing of pristine and diagenetic material (Banner 1995). In general, in the dataset presented, different shells from the same bed, most of which passed the steps of the diagenetic screening, have $^{87}Sr/^{86}Sr$ ratios within a very narrow range, slightly higher than the analytical precision (2 s.e. 0.000007). This internal consistency of the Sr-isotope ratios of different samples from the same level can be considered as strong evidence that the samples used for strontium-isotope stratigraphy retained their original marine Sr-isotope signature (McArthur 1994, McArthur et al. 2006, Brand et al. 2011).

Sample B1-B has a Sr concentration below the threshold here adopted whereas for sample B1-C we could not get enough material to perform both ICP and Sr-isotope measurements. However, these samples exhibit $^{87}Sr/^{86}Sr$ ratios very similar to that from sample B1-A and significantly lower than the isotopic ratio of the micritic matrix enclosing the shells (Table 1A). Accordingly, these shells are considered to preserve the original

^{87}Sr/^{86}Sr signal and are used for strontium-isotope stratigraphy. On the other hand, samples C1-A, C1-B and A3-A were discarded despite of their high Sr concentration because of their Fe and Mn values, which were above the chosen limit and mainly because their ^{87}Sr/^{86}Sr ratios were found to be considerably higher than the ratio measured in the other samples from the same stratigraphic level (Table 1A). Finally, sample C1-C was used for strontium-isotope stratigraphy despite its Fe and Mn concentrations above the indicated threshold since this sample yielded the lowest ^{87}Sr/^{86}Sr ratio of the level (Table 1A). However, it cannot be ruled out that the original ^{87}Sr/^{86}Sr of this sample could have been, in part, modified by diagenesis and therefore the derived SIS ages for this level are treated in a conservative way (see below).

5. Strontium ratios and derived numerical ages of the samples

The ^{87}Sr/^{86}Sr values obtained from low-Mg calcite shells collected for the present study in the Maestrat Basin range from 0.707488 ± 0.000009 down to 0.707310 ± 0.000007 (Table 1A). These values translate respectively into numerical ages of 127.49-128.33 Ma (+1.44/–0.88) and 118.93 Ma (+0.73/–0.7), which constrain the age of the specimens analysed within the Barremian-early Late Aptian time interval (GTS 2004). For description of the Sr-isotopic data and the derived numerical ages presented in Table 1B refer to Pascual-Cebrian (2014).

The oldest shells studied are found in the Artoles Formation (samples A1 and A2 from its lower-middle part and sample A3 from its upper part). The Sr-isotope ratios of the two sampled intervals are identical (0.707488 ± 0.000009) and translate into a numerical age of 127.49-128.33 Ma (+1.44/–0.88) corresponding to the early Late Barremian (Fig. 3 and Table 1A). However, if the total age range is considered (126.61-129.77 Ma), the age of the samples spans almost the whole Barremian (see GTS 2004). Such a large age interval is due to the fact that the Sr-isotope curve from the middle Early Barremian to the early Late Barremian is characterized by fairly stable values (e.g., Bodin et al. 2009; Mutterlose et al. 2014). In southeastern France, Bodin et al. (2009) report mean ^{87}Sr/^{86}Sr ratios of 0.707488 to 0.707506 for this interval (*Kotetishvilia Nicklesi* through *Toxancyloceras vandenheckii* Tethyan ammonite zones). These values are slightly higher than those reported for the Early Barremian to the early Late Barremian by McArthur et al. (2004) from the Boreal realm (~0.707475 in the Early Barremian *Hoplocrioceras rarocinctum* Zone to 0.707485 in the lowermost early Late Barremian *Parancyloceras elegans* Zone). Furthermore, as highlighted by Mutterlose et al. (2014), an offset between the Tethyan and Boreal Sr-isotopic curves from the middle Early Barremian to the early Late Barremian makes it difficult to use strontium-isotope stratigraphy for precise age calculation across this interval. However, if we consider the absolute Sr-isotopic values of our samples as a tool of correlation, they are indistinguishable from those of Bodin et al. (2009) and McArthur et al. (2004) constraining the age of our samples A to the middle Early-early Late Barremian. The Artoles Formation in the Salzedella sub-basin (Fig. 1B; depocentre of the Maestrat Basin) is about 750 m-thick. Samples A1 and A2 were collected in the lower-middle part of this formation in the depocentre of the basin, about 300 meters above the last Hauterivian ammonite. This would suggest a middle/late Early Barremian age for samples A1 and A2. On the other hand, sample A3 collected in the upper part of the Artoles Formation is ascribed to the early Late Barremian.

The ^{87}Sr/^{86}Sr ratio of 0.707466 ± 0.000013 for samples C1 from the lower part of the Cervera del Maestrat Formation translates into an age of 126.24 Ma (+0.77/–0.62) (Fig. 3 and Table 1A). This numerical age is coincident with the Late Barremian by reference to the GTS2004. Furthermore, the ^{87}Sr/^{86}Sr values from our samples C1 (0.707466, 0.707513 and 0.707565; Table 1A) are similar to the mean ^{87}Sr/^{86}Sr values reported by Bodin et al. (2009) in southeastern France for the Late Barremian *Gerhardtia Sartusiana* to *Imerites giraudi* ammonite zones (0.707466 and 0.707452, respectively). However, owing to the concerns raised in the previous section, the mean $^{87}Sr/^{86}Sr$ ratio of samples C1 is regarded as a maximum age estimate. In fact, considering the marine Sr reference curve of McArthur et al. (2001) for the Barremian-Aptian interval, any lower $^{87}Sr/^{86}Sr$ ratio from this stratigraphic level than that of sample C1-C would translate into younger ages.

The $^{87}Sr/^{86}Sr$ value of 0.707425 ± 0.000013 obtained from the upper part from the Xert Formation (samples X1), gives an age of 124.94 Ma (+0.59/–0.64) (Fig. 3 and Table 1A). This numerical age and the associated minimum to maximum range are in accordance with a latest Barremian-earliest Aptian age (GST2004).

The youngest low-Mg calcite shells analysed are those collected in the Benassal Formation (samples B1). Sr-isotopic data obtained for this latter lithostratigraphic unit yield a mean $^{87}Sr/^{86}Sr$ value of 0.707310 ± 0.000007, translating into an age of 118.93 Ma (+0.73/–0.7) (Fig. 3 and Table 1A). This numerical age range corresponds to the early Late Aptian (GST2004).

---------------- Table 1 (LANDSCAPE ORIENTATION - width of page) near here --------------

6. New ammonoid biostratigraphic data

In November 2014, an ammonite identified as a *Martelites* sp. (Fig. 9) was collected by the authors of this study in the lower part of the Xert Formation in Torre Miró (km. 70 of the N-232 road; UTM coordinates: X=30T 747624, Y= 4508200), in the Morella sub-basin (Fig. 1B). The ammonite was found above the contact between the Morella and Xert formations (Fig. 3). *Martelites* sp. belongs to the *Martelites sarasini* Zone (Late Barremian), particularly to the lower part of the *Martelites sarasini* Subzone of the standard

Mediterranean zonation found in Reboulet et al. (2014). This finding constitutes the first quotation of this genus in the Maestrat Basin and allows a precise age calibration of the lower part of the Xert Formation. A Late Barremian age for the lower part of the Xert Formation is in agreement with the strontium-isotopic data presented in this work (samples X1; Fig. 3 and Table 1A).

---------------------------------- Figure 9 (width of page) near here ----------------------------------

7. Major transgressive-regressive cycles

The Barremian-Early Albian sedimentary record of the Maestrat Basin is here subdivided into six long-term transgressive-regressive sequences for comparison with other coeval marine basins (Fig. 3). The hierarchy of the sequences described is considered as high rank, as lower-rank stratigraphic units and surfaces are nested within them. Based on the numerical ages derived from Sr-isotope ratios in Table 1, and the ammonoid biostratigraphic data from the Maestrat Basin tied to the GTS2004 shown in Fig. 3, the duration of the high-rank cyclic variations in depositional trends characterized is consistent with the second- (3–50 Ma) and third-order (0.5–3 Ma) relative sea-level cycles of Vail et al. (1991).

The transgressive unit of the first sequence corresponds to the marine limestones and marls of the Artoles Formation (Figs 3, 5A and 6A). The Artoles Formation is a diachronous unit (Salas 1987, Salas et al. 2001). Its base is older in the basin depocentre (Salzedella sub-basin; Fig. 1B), where it overlies the Hauterivian platform carbonates of the Llàcova Formation (Salas 1987), and younger in the more marginal settings of the Maestrat Basin (Penyagolosa, Galve, El Perelló and Morella sub-basins; Fig. 1B), where it locally onlaps the continental clastics of the Camarillas Formation (Figs 5A and 6A) or the lacustrine limestones and marls of the Cantaperdius Formation (Fig. 3; Salas 1987). The Camarillas and Cantaperdius formations are Barremian in age (e.g., Canérot et al. 1982; Salas 1987; Salas et al. 2001). The regressive strata of the first sequence are represented by the tidal-influenced marine deposits of the upper part of the Artoles Formation (Figs 5A and 6A), the continental clastics of the Morella Formation (Figs 5A-B) and its coastal to marine equivalent, the Cervera del Maestrat Formation (Figs 5C and 6A). The boundary between the transgressive and regressive deposits of Sequence I is located within the Artoles Formation and corresponds to a maximum-flooding surface (Figs 5A and 6A), which lacks numerical dating (Fig. 3), and coincides with the downlap surface of tidal-influenced normal regressive strata above a thick marly unit (Fig. 5A). This first transgressive-regressive sequence is Barremian in age and had a duration of about 3-4 My (Fig. 3).

The onset of the second major transgressive-regressive sequence of relative sea level is marked by a transgressive surface located at the uppermost part of the Morella Formation, where the characteristic continental red clays and sandstones of this formation change into coastal and shallow-marine clastics (Figs 3 and 5A-B). The siliciclastic-influenced deposits of the lower part of the Xert Formation, the limestones with *Palorbitolina lenticularis* of the upper part of the Xert Formation, and the overlying basinal marls and limestones of the Forcall Formation constitute the rest of the transgressive unit of this second sequence (Figs 5A, 6 and 7A-C). The prograding platform carbonates with rudist bivalves and corals of the Villarroya de los Pinares Formation characterize the regressive strata of the sequence (Figs 6 and 7A, C). The maximum-flooding surface of the sequence coincides with the downlap surface exhibited by the normal regressive clinoforms of this latter formation (Bover-Arnal et al. 2009, 2011a, 2014, 2015). This second long-term regressive unit, was terminated by subaerial exposure and local incision of the platform carbonates of the Villarroya de los Pinares Formation (Vennin and Aurell 2001, Bover-Arnal et al. 2009, 2010, 2014, 2015, Embry et al. 2010). The carbonate platforms of the Villarroya de los Pinares Formation pass basinwards into the marls of the Forcall Formation (Fig. 3; Bover-Arnal et al. 2009, 2010, 2014, 2015). This second transgressive-regressive sequence spanned the latest Barremian-latest Early Aptian time interval and had a duration of around 5 My (Fig. 3).

The lower part of the transgressive unit of the third sequence corresponds to peritidal to shallow subtidal deposits back-filling erosional incisions and retrograding platform carbonates belonging to the Villarroya de los Pinares Formation (Bover-Arnal et al. 2009, 2014, 2015). In the course of this major transgressive event, the platform carbonates of the Villarroya de los Pinares Formation were drowned and buried by marls belonging to the lower part of the Benassal Formation (Figs 3, 6A, 7A, 7C-D and 8B; Bover-Arnal et al. 2009, 2014, 2015). The establishment of prograding carbonate platforms with rudists and corals (Benassal Formation), which pass basinwards into marls, marks the regressive stage of the third sequence. These platform carbonates were locally subaerially exposed and incised (Fig. 3; Bover-Arnal et al. 2014). The change in stratal stacking pattern from transgressive marls to normal regressive carbonate platforms is marked by a maximum-flooding surface (Figs 6A, 7A, 7C-D and 8B). This third transgressive-regressive cycle spanned the latest Early Aptian-early Late Aptian with a duration of ~3 My (Fig. 3).

Transgressive-regressive Sequence IV commences with peritidal to shallow subtidal strata back-filling the erosional incisions formed during the latest regressive stage of the third sequence (Bover-Arnal et al. 2014), and with backstepping of platform carbonates. These carbonate platforms were drowned in the course of the transgression evolving upwards into marly deposits (Figs 3, 6A and 8B; Bover-Arnal et al. 2010). The boundary between the transgressive and normal regressive deposits of the sequence correponds to a maximum-flooding surface, which is placed at the contact between the underlying marly interval and the overlying prograding carbonates, which are rich in orbitolinids, rudists bivalves and corals (Bover-Arnal et al. 2010). The time span of this sequence would be around 4 My.

The transgressive unit of Sequence V lacks precise age dating (Figs 3, 6A and 87B). However, it is interpreted to be coeval with the occurrence of the ammonoid specimen *Acanthohoplites bergeroni* in the Galve and Oliete sub-basins (Figs 1B and 3; Weisser 1959, Martínez et al. 1994, Garcia et al. 2014). The regressive unit of the fifh sequence is distinguished by punctuated episodes of carbonate platform development and a progressive change to more coastal and transitional deposits in the uppermost part of the Benassal Formation (Figs 6A and 8B). These regressive strata correspond to intertidal reddish sandstones, sandy limestones and clays, which correspond to the uppermost part of the Benassal Formation (Figs 6A and 8B). Therefore, the time span of sequence V would be *c.* 2.5 My (Fig. 3).

The subsequent transgressive event (Sequence VI) is marked by the coastal and transitional clastic and coal deposits of the lower part of the Escucha Formation (Figs 3 and 7C). In the Salzedella sub-basin (Fig. 1B), which corresponds to the depocentre of the Maestrat Basin, the lower part of the Escucha Formation contains Albian ammonoids (Moreno-Bedmar et al. 2008, Garcia et al. 2014; Fig. 3). The maximum-flooding zone of this transgressive unit is interpreted to correspond to the stratigraphic position of the *Douvilleiceras* ammonoids (Fig. 3). Accordingly, this transgressive unit would have spanned around 1.5 My.

Lower-rank changes of relative sea level were superimposed onto the high-rank cycles, reflecting the activity of local tectonics and intra-basinal differences in the rates of sediment input/production and accummulation. In the northern part of the Salzedella sub-basin (central Maestrat Basin; Fig. 1B), where the base of the Barremian consists of lacustrine limestones and marls belonging to the Cantaperdius Formation, two lower-rank transgressive-regressive sequences equivalent to Sequence I were characterized by Salas (1987). Within the transgressive unit of Sequence II, three conspicuous lower-rank regressive events have been recognized in certain areas of the basin. A higher-frequency regression is recorded at the uppermost part of the Xert Formation in the Galve sub-basin (Fig. 1B; Vennin and Aurell 2001, Bover-Arnal et al. 2010, Embry et al., 2010). The metre-thick and massive beds of limestones with *Palorbitolina lenticularis* found at the lower-middle part of the Forcall Formation, the so-called 'Barra de Morella' (Canérot et al. 1982, Moreno-Bedmar et al. 2010), also indicate a lower-rank regression of relative sea level within the high-rank transgressive context. The coral-rubble deposits encrusted by *Lithocodium aggregatum* found in the marls of the Forcall Formation cropping out in the Galve sub-basin (Fig. 1B; Bover-Arnal et al. 2010, 2011b, Schlagintweit et al. 2010, Schlagintweit and Bover-Arnal et al. 2012, 2013), are also consistent with a higher-frequency shallowing of relative sea level.

The three well-developed high-rank transgressive-regressive sequences of the Benassal Formation (sequences III, IV and V) have been recognized only in certain areas of the western part of the Maestrat Basin, in the Penyagolosa and Galve sub-basins (Figs 1B, 6A and 8B; e.g., Martín-Martín et al. 2013). In other areas of the basin, including the northern and eastern parts of the Galve sub-basin (Fig. 1B), only two transgressive-regressive sequences were identified in the Benassal Formation (e.g., Bover-Arnal et al. 2010).

8. Discussion

8.1. Implications for the Barremian-Early Albian chronostratigraphy of the Maestrat Basin

The numerical ages obtained from the strontium-isotope ratios measured in this study (Fig. 3 and Table 1), as well as the recent *Martelites* sp. finding (Fig. 9), result in the reevaluation of the chronostratigraphy of the Artoles, Morella, Cervera del Maestrat and Xert formations. The last three lithostratigraphic units, which have been classically interpreted to be of Early Aptian age (e.g., Canérot et al. 1982, Salas 1987, Salas et al. 1995, 2001, Clariana et al. 2000, Vennin and Aurell 2001, Gàmez et al. 2003, Yagüe et al. 2003, Liesa et al. 2006, Canudo et al. 2008a, b, Jorquera-Grau et al. 2009, Bover-Arnal et al. 2009, 2010, Moreno-Bedmar et al. 2009, 2010, Pérez-García et al. 2009, 2014, Embry et al. 2010, Gasulla et al. 2011a, 2011b, 2012), are here ascribed to the Late Barremian (Figs 2 and 3). However, the $^{87}Sr/^{86}Sr$ values of the samples X1 collected at the uppermost part of the Xert Formation give an age of 124.94 Ma (+0.59/–0.64) (Fig. 3 and Table 1). As the base of the Aptian is at about 125 Ma (GTS2004), an earliest Aptian age for the uppermost part of the Xert Formation cannot be ruled out. Along the same lines, the results sustain a middle/late Early Barremian age for the lower-middle part of the Artoles Formation (samples A1 and A2; Fig. 3 and Table 1), and an early Late Barremian age for its upper part (samples A3), which has been commonly interpreted to be partly Early Aptian in age (e.g., Salas 1987, Salas et al. 1995, 2001, Vennin and Aurell 2001, Caja 2004, Liesa et al. 2006, Embry et al. 2010). The age of the lowermost stratigraphic interval of the Artoles Formation was not investigated in this study. Nevertheless, given that the boundary between the Early and the Late Barremian is dated at about 128.3 Ma (GST2004), the numerical age of 127.49-128.33 Ma obtained from samples A1 and A2 (Fig. 3 and Table 1), which were collected from the lower-middle part of the Artoles Formation, constrains the lower stratigraphic interval of this formation to the Early Barremian. Additionally, the uppermost part of the marls and limestones of La Gaita Formation, which is situated stratigraphically below the Artoles and Llàcova formations in the Salzedella sub-basin (depocentre of the Maestrat Basin; Fig. 1B; Salas et al. 2001), contains latest Hauterivian ammonites belonging to the *Pseudothurmannia ohmni* Zone (Garcia et al. 2014).

The basal part of the Forcall Formation lacks an ammonite record or strontium-stratigraphic constraints (Fig. 3 and Table 1). It could be either terminal Barremian or earliest Aptian. Nevertheless, the base of the first Early Aptian ammonite zone (*Deshayesites oglanlensis*; Reboulet et al. 2011, 2014) seems to be recorded in the lowermost (but not basal) part of the Forcall Formation (Moreno-Bedmar and Garcia 2011), where specimens of *Deshayesites antiquus* occur (Fig. 3). The rest of the Forcall Formation is of Early Aptian age (Moreno-Bedmar et al. 2009, 2010, Bover-Arnal et al. 2010, Garcia et al. 2014). In consequence, in the Maestrat Basin, the Barremian-Aptian boundary is located within the stratigraphic interval comprised by the uppermost part of the Xert Formation and the lowermost part of the marls of the Forcall Formation, most likely at the lowermost, non-basal part of this latter lithostratigraphic unit (Fig. 3).

The ages of the Villarroya de los Pinares and Benassal formations are not modified with respect to recent publications (e.g., Bover-Arnal et al. 2012, 2014, 2015, Moreno-Bedmar et al. 2012, Garcia et al. 2014, Pascual-Cebrian 2014). The Villarroya de los Pinares Formation is confirmed to be Early Aptian in age, whereas the Benassal Formation spans the latest Early Aptian-Late Aptian time interval (Fig. 3 and Table 1). A preliminary biostratigraphic analysis based on orbitolinid foraminifera carried out in the Benassal Formation of the Benicàssim area (Penyagolosa sub-basin; Fig. 1B) suggests that, in this particular locality, the top of this lithostratigraphic unit could be as young as Albian (Martín-Martín et al. 2013). However, further study is necessary to confirm these results.

The age of the long-term sea-level falls, which resulted in subaerial exposure and incision of the platform carbonates in the upper part of the Villarroya de los Pinares Formation (Bover-Arnal et al. 2009, 2010, 2011a, 2015) and the lower part of the Benassal Formation (Bover-Arnal et al. 2014) can be also precisely calibrated now. These two major sea-level drops occurred respectively within the *Dufrenoyia furcata* Zone (late Early Aptian) and the upper part of the *Epicheloniceras martini* Zone (early Late Aptian) (Fig. 3 and Table 1). Based on the numerical ages of the GTS2004, and in accordance with the ammonite occurrences in the basin and the numerical ages derived from $^{87}Sr/^{86}Sr$ values measured in samples B1 (Fig. 3 and Table 1), which were collected within the back-filling deposits of the incised valley found in the lower part of the Benassal Formation in the Morella sub-basin (see Bover-Arnal et al. 2014; Figs 1B and 3), the duration of the stratigraphic gaps associated with these subaerial unconformities would be much less than 1 My (Fig. 3). However, the duration of each of these stratigraphic gaps probably varied across the basin.

In this regard, the stratigraphic record can be particularly incomplete in specific parts of the basin due to non-deposition (see Figs 6 and 9 in Salas et al. 2001) or due to ancient and/or present-day erosion. For instance, the Morella Formation is recorded in the central part of the Galve sub-basin (Figs 1B and 5A) but was not deposited in the eastern part of it (Bover-Arnal et al. 2010). The Albian Escucha Formation, as well as Miocene deposits, are locally found above erosional uncoformities affecting the underlying sedimentary record down to the Late Triassic (e.g., Salas 1987, Querol 1990, Solé de Porta et al. 1994, Salas et al. 1995).

The lithologies and fossil distributions represented in Fig. 3 are the most common and significant. Main lateral changes in lithology at the scale of formations occurring throughout the basin are also shown in Fig. 3. For example, the continental part of the Morella Formation (Figs 5A-B) passes laterally (seawards) to its coastal to shallow-marine equivalent, the Cervera del Maestrat Formation (Figs 3 and 5C). The Villarroya de los Pinares Formation is missing in basinal settings due to the lateral transition from platform carbonates to the basinal marls of the Forcall Formation and/or to the marls of the lowermost part of the Benassal Formation (Fig. 3; Bover-Arnal et al. 2009, 2011a, 2014, 2015). The platform carbonates belonging to the Benassal Formation fade into basinal marls, which are included within the same formation (Fig. 3; Bover-Arnal et al. 2010, 2014).

Moreover, the lithostratigraphic units assessed, particularly the Artoles, Forcall and Villarroya de los Pinares formations, are diachronous across the basin. For instance, the Forcall Formation, which records the four Early Aptian ammonoid zones in the Galve and Morella sub-basins, only spans the *Deshayesites forbesi* Zone in the Oliete sub-basin (Moreno-Bedmar et al. 2010, Garcia et al. 2014). Another case of diachronism is known from the eastern part of the Galve sub-basin (Fig. 1B), where the Villarroya de los Pinares Formation spans part of the *Deshayesites deshayesi* and *Dufrenoyia furcata* zones (Bover-Arnal et al. 2010, 2012), whereas in the central part of this sub-basin, as well as in the Morella sub-basin (Fig. 1B), the Villarroya de los Pinares Formation is latest Early Aptian in age (intra *Dufrenoyia furcata* Zone) (Bover-Arnal et al. 2010, 2014, 2015). The diachroneity of the Artoles Formation is explained in section 7 of this paper.

The last controversial issue regarding the Barremian-Early Albian chronostratigraphy of the Maestrat Basin is the age of the lowermost part of the Escucha Formation, which has been ascribed either to the Late Aptian (e.g., Boulouard and Canérot 1970, Peyrot et al. 2007, de Gea et al. 2008) or to the Early Albian (e.g., Querol 1990, Querol et al. 1992, Martínez et al. 1994, Solé de Porta and Salas 1994, Solé de Porta et al. 1994, Moreno-Bedmar et al. 2008). See also Villanueva-Amadoz et al. (2010) for a review on the different age assignments of the lower part of the Escucha Formation. Besides the fact that the basal part of the Escucha Formation is probably diachronous across the basin (e.g., Canérot et al. 1982), in areas where the base of the Escucha Formation is not marked by an unconformity (Canérot et al. 1982, Salas 1987, Querol 1990, Querol et al. 1992, Salas et al. 1995), the passage from the underlying marine limestones and marls of the Benassal Formation to the marine limestones, marls, sandstones, lutites and coals of the lower part of the Escucha Formation is progressive and the limit between these two formations is difficult to establish. Thus, the same stratigraphic interval may be arbitrarily ascribed to the uppermost part of the Benassal Formation or to the lowermost part of the Escucha Formation by different authors. This fact probably also accounts for the different age assignments reported for the base of the Escucha Formation in the literature. In this paper, however, the age of the lowermost part of the Escucha Formation is ascribed to the Early Albian following the ammonite findings reported from the depocentre of the Maestrat Basin (Martínez et al. 1994, Moreno-Bedmar et al. 2008), in the Salzedella sub-basin (Fig. 1B) where the Escucha Formation is thus most expanded.

Accordingly, the Barremian-Early Albian chronostratigraphic framework for the Maestrat Basin summarized in Fig. 3 depicts a general pattern, which can be tracked across most of the basin. However, this general chronostratigraphic model may show inherent variations due to local tectono-sedimentary particularities.

8.2. Tethyan significance of the Barremian-Aptian evolution of the Maestrat Basin

The updated chronostratigraphic framework for the Barremian-Early Albian succession from the Maestrat Basin presented herein allows a more precise correlation with coeval sedimentary records from other basins of the Tethys. The Barremian-Aptian boundary in the Maestrat Basin can now be located at around the contact between the Xert and Forcall formations (Fig. 2), most likely in the lowermost, non-basal part of the Forcall Formation (Figs 2 and 3). The assignment of the basal part of the transgressive marls of the Forcall Formation to the latest Barremian is in agreement with the age of the base of marly transgressive deposits recorded in other basins of the Tethys.

In this respect, in the area of Cassis-La Bédoule, in the South Provence Basin (SE France), Late Barremian ammonites of the genera *Pseudocrioceras* and *Martelites* are found at the base of a basinal marl-limestone alternation (Delanoy et al. 1997, Ropolo et al. 1999, 2000), which overlies the Urgonian carbonates of the Provence Platform. The top of these limestones of the Provence Platform at Cassis-La Bédoule is marked by a drowning discontinuity (Masse and Fenerci-Masse 2011). This scenario is comparable to that described in the Maestrat Basin where the Late Barremian platform carbonates of the Xert Formation were drowned in the terminal Barremian and overlain by the basinal marls of the Forcall Formation (Fig. 3). Similarly, in Cassis-La Bédoule, the Barremian-Aptian boundary is also located in the lower, non-basal part of the transgressive basinal marly-limestone unit (Delanoy et al. 1997, Ropolo et al. 1999, 2000).

Other examples are found in the Basque-Cantabrian Basin (N Spain), where continental deposits of the Wealden series are overlain by marine marls of the Errenaga Formation. García-Mondéjar et al. (2009) report the presence of the ammonite *Valdedorsella* sp. at the base of this transgressive marly unit, and ascribe this genus to the latest Barremian. Along the same lines, in the Organyà Basin (S Pyrenees), the base of the basinal marls of the Cabó Formation is characterized by an ammonite record that includes *Pseudocrioceras waagenoides* and *Acrioceras* sp., and thus belongs to the *Pseudocrioceras waagenoides* Sub-zone of the *Imerites giraudi* Zone (Late Barremian) (Moreno-Bedmar 2010, Moreno-Bedmar and Garcia 2011). Below the marly transgressive deposits of the Cabó Formation, Valanginian to Barremian platform carbonates belonging to the Prada Formation are found (Bernaus et al. 2002, 2003).

Therefore, in the Maestrat Basin, the passage from the Barremian into the Aptian occurred in the course of a wide transgression, which started in the Late Barremian and ended within the Early Aptian. This Late Barremian-Early Aptian major transgressive event (Sequence II) drowned the carbonate systems corresponding to the Xert Formation (Fig. 3), as well as coeval carbonate platforms from nearby basins (e.g., Masse and Fenerci-Masse 2011), within the terminal Barremian. In addition, according to the GTS2004, the Late Barremian-Early Aptian marine transgression lasted between 3 and 4 My (Fig. 3) and thus would be in agreement with a second-order (*sensu* Vail et al., 1991) eustatic event. The acme of this major transgression occurred within the Early Aptian (Fig. 3; e.g., Bover-Arnal et al. 2010). As a matter of fact, transgressive deposits of Early Aptian age are widespread along the margins of the Tethys ocean (e.g., Föllmi et al. 1994, Sahagian et al. 1996, Hardenbol et al. 1998, Wissler et al. 2003, Husinec and Jelaska 2006, Hfaiedh et al. 2013, Suarez-Gonzalez et al. 2013, Pictet et al. 2015).

Sample F1 corresponds to a shell of a polyconitid rudist collected at the lower part of the Forcall Formation in the Galve sub-basin within a coral rubble horizon encrusted by *Lithocodium aggregatum* (Schlagintweit et al. 2010, Bover-Arnal et al. 2011b). This coral rubble level is coeval with the OAE1 (Moreno-Bedmar et al. 2009, Bover-Arnal et al. 2010); more exactly with the global positive C-isotope excursion characterized as the segment C4 by Menegatti et al. (1998) (see Cors et al. 2015). The $^{87}\text{Sr}/^{86}\text{Sr}$ ratio obtained from this sample translates into a numerical age of 123.6 Ma (+0.53/−0.57) (Fig. 3 and Table 1). This gives a rough age of the positive excursion of the carbon-isotope values correlatable with the segment C4 of Menegatti et al. (1998), and of the OAE1a itself in this basin.

On the other hand, the location of the Barremian-Aptian boundary within the stratigraphic interval spanning the lowermost section of the Forcall Formation ascribes the first *Palorbitolina lenticularis* occurrences recorded at the upper part of the Xert Formation (e.g., Salas 1987, Vennin and Aurell 2001, Bover-Arnal et al. 2010, Embry et al. 2010) to the Late Barremian (Fig. 3), and not the Early Aptian as previously thought (Fig. 2). In this respect, the Late Barremian age of the oldest *Palorbitolina lenticularis* blooms found in the Maestrat basin is consistent with other first occurrences identified in other Tethyan regions such as the Arabian Plate (e.g., Schroeder et al. 2010), the Pyrenees (e.g., Bernaus et al. 2002, 2003), the Helvetic Nappes (e.g., Stein et al. 2012), the Provence Platform in SE France (e.g., Leonide et al. 2012) or the French Subalpine Chains (e.g., Huck et al. 2013). Furthermore, *Palorbitolina lenticularis* mass-occurrences are also recorded within the Early Aptian Forcall Formation in the Maestrat Basin (e.g., Schroeder 1964, Canérot et al. 1982, Bover-Arnal et al. 2010, 2011b, 2014), as well as in other Early Aptian deposits of the Tethys and the Atlantic extension of it (e.g., Arnaud and Arnaud-Vanneau 1991, Vilas et al. 1995, Husinec et al. 2000, Burla et al. 2008, Schroeder et al. 2010, Leonide et al. 2012).

The major transgressive-regressive sequences interpreted for the Barremian-Early Albian succession of the Maestrat Basin are next compared to the sequences compiled by Hardenbol et al. (1998) from the European basins of the Tethys (Fig. 3). These sequences of Hardenbol et al. (1998) were tied to numerical ages by Gradstein et al. (2004), as done in the present study with the interpreted major Barremian-Early Albian transgressive-regressive sequences. Sequence I (Figs 5A and 6A) comprises the Barr1, Barr2, Barr3, Barr4 and Barr5 sequences of Hardenbol et al. (1998) and thus, there is not a fit between them (Fig. 3). Sequence II (Figs 3, 5A-B, 6 and 7A, C) comprises the sequences Barr6, Ap1, Ap2 and Ap3 of Hardenbol et al. (1998). The acme of the transgression related to Sequence II occurred around the boundary between the *Deshayesites forbesi* and *Deshayesites deshayesi* zones (Fig. 3) as also marked by Gradstein et al. (2004). The regression of Sequence II spans most of the *Deshayesites deshayesi* and *Dufrenoyia furcata* zones (Fig. 3), also throughout the Tethys (Gradstein et al. 2004). Sequence III (Figs 3, 6A, 7A, D and 8B) fits rather well with the sequence Ap4 of Hardenbol et al. (1998). The start of the transgression of Sequence IV (Figs 3, 6A and 8B) is rather coeval with the transgression of sequence Ap5 (Gradstein et al., 2004). However, the regression of Sequence IV (Figs 3, 6A and 8B) is not correlatable with the regressive part of the sequence Ap5 of Hardenbol et al. (1998). The transgressive part of Sequence V is coeval with the acme of the transgression corresponding to the sequence Ap5 of Hardenbol et al. (1998) (Fig. 3). The start of the regression of Sequence V is correlatable to the regression of sequence Ap5 (Fig. 3). On the other hand, global sequences Ap6, Al1 and Al2 do not show any pattern comparable to the major transgressive-regressive sequences characterized in the Maestrat Basin (Fig. 3). However, the onset of transgression during Sequence VI is correlatable with the upper part of the transgression of sequence Ap6 (Fig. 3). Accordingly, sequences II and III (Figs 3, 5A-B, 6, 7A, 7C-D and 8B), as well as the transgressive parts of sequences IV and V, the start of the regression of Sequence V, and the onset of transgression of Sequence VI (Figs 3, 6A and 8B), seem to have responded to a eustatic signal of Tethyan significance.

9. Conclusions

According to the numerical ages derived from strontium-isotope data and the new ammonoid finding presented in this study, the Aptian Stage in the Maestrat Basin began within the stratigraphic interval comprised between the uppermost part of the Xert Formation and the lowermost part of the Forcall Formation. In this study, by analogy with the ammonoid-calibrated latest Barremian age of the basal part of the transgressive marl successions recorded in the nearby Vocontian, Organyà and Basque-Cantabrian basins, the stratigraphic location of the Barremian-Aptian boundary within the lowermost, non-basal part of the marly transgressive deposits of the Forcall Formation is favoured.

The new chronostratigraphic considerations presented in this paper indicate that: i) the dinosaur and other vertebrate remains of the Morella Formation and the lowermost part of the Xert Formation are of Late Barremian age, ii) the first *Palorbitolina lenticularis* blooms recorded in the upper Xert Formation are Late Barremian in age, iii) in the Maestrat Basin, the Aptian began in the course of a major transgression, which was accompanied by the proliferation of *Palorbitolina lenticularis* along the margins of the Tethys, iv) this transgressive event started in the latest Barremian and drowned terminal Barremian carbonate platforms (Xert Formation) throughout the basin, v) extensive carbonate platforms recovered coevally with a post-OAE1a late Early Aptian major regression of relative sea level, spanning the upper part of the *Deshayesites deshayesi* Zone and most of the *Dufrenoyia furcata* Zone, vi) these carbonate platforms, which belong to the rudist- and coral-bearing Villarroya de los Pinares Formation, terminated with subaerial exposure or drowning within the uppermost *Dufrenoyia furcata* Zone (latest Early Aptian), vii) a second episode of rudist- and coral-dominated carbonate platform development occurred in the upper part of the *Epicheloniceras martini* Zone (early Late Aptian), viii) these carbonate platforms correspond to the Benassal Formation and were terminated due to emersion or drowning within the time interval spanning the uppermost part of the *Epicheloniceras martini* Zone and the lowermost part of the *Parahoplites melchioris* Zone (early Late Aptian), and ix) punctuated and minor episodes of carbonate platform growth occurred during the latest Aptian, gradually evolving into more coastal and transitional deposits in the uppermost part of the Benassal Formation, which is overlain by Early Albian clastic and coal deposits corresponding to the Escucha Formation.

Acknowledgements

We are especially grateful to André Strasser, Peter W. Skelton and to an anonymous reviewer for their helpful comments and suggestions on the manuscript. Jordi Illa and Alejandro Gallardo are greatly thanked for laboratory assistance. We are grateful to José Miguel Gasulla for inviting us to visit a quarry pit where the Morella Formation is mined and allowing us to take the picture shown in Fig. 5B. Prof. Juan Diego Martín-Martín kindly provided the panoramic photo of the Orpesa Range shown in Fig. 8A. This study was financed by the I+D+i research project CGL2008-04916, the Consolider-Ingenio 2010 programme, under CSD 2006-0004 “Topo-Iberia”, and the Grup de Recerca Reconegut per la Generalitat de Catalunya 2014 SGR 251 “Geologia Sedimentària”.

References

Aguilar, M.J., Ramírez del Pozo, J., Riba, O., 1971. Algunas precisiones sobre la sedimentación y paleoecología del Cretácico inferior en la Zona de Utrillas-Villarroya de los Pinares (Teruel). Estudios Geológicos **27**, 497–512.

Al-Aasm, I.S., Veizer, J., 1986. Diagenetic stabilization of aragonite and low-Mg calcite. I. Trace elements in rudists. Journal of Sedimentary Petrology **56**, 763–770.

Arnaud, H., Arnaud-Vanneau, A., 1991. Les calcaires Urgoniens des massifs subalpins septentrionaux et du Jura (France): âge et discussion des données stratigraphiques. Géologie Alpine **67**, 63–79.

Banner, J.L., 1995. Application of the trace element and isotope geochemistry of strontium to studies of carbonate diagenesis. Sedimentology **42**, 805–824.

Bachmann, M., Hirsch, F., 2006. Lower Cretaceous carbonate platform of the eastern Levant (Galilee and the Golan Heights): stratigraphy and second-order sea-level change. Cretaceous Research **27**, 487–512.

Bernaus, J.M., Arnaud-Vanneau, A., Caus, E., 2002. Stratigraphic distribution of

Valanginian–Early Aptian shallow-water benthic foraminifera and algae, and depositional sequences of a carbonate platform in a tectonically-controlled basin: the Organyà Basin, Pyrenees, Spain. Cretaceous Research **23**, 25–36.

Bernaus, J.M., Arnaud-Vanneau, A., Caus, E., 2003. Carbonate platform sequence stratigraphy in a rapidly subsiding area: the Late Barremian–Early Aptian of the Organyà basin, Spanish Pyrenees. Sedimentary Geology **159**, 177–201.

Bodin, S., Fiet, N., Godet, A., Matera, V., Westermann, S., Clément, A., Janssen, N.M.M., Stille, P., Föllmi, K.B., 2009. Early Cretaceous (late Berriasian to early Aptian) palaeoceanographic change along the northwestern Tethyan margin (Vocontian Trough, southeastern France): $\delta^{13}C$, $\delta^{18}O$ and Sr-isotope belemnite and whole-rock records. Cretaceous Research **30**, 1247–1262.

Boix, C., Frijia, G., Vicedo, V., Bernaus, J.M., Di Lucia, M., Parente, M., Caus, E., 2011. Larger foraminifera distribution and strontium isotope stratigraphy of the La Cova limestones (Coniacian–Santonian, "Serra del Montsec", Pyrenees, NE Spain). Cretaceous Research **32**, 806–822.

Bonilla-Rodríguez, A.J., González, L.A., Douglas Walker, J., Santos, H., 2014. Strontium isotope ($^{87}Sr/^{86}Sr$) stratigraphy from the *Coalcomana–Caprinuloidea* rudist assemblage in the Greater Antilles (Puerto Rico, Dominican Republic and Jamaica). Cretaceous Research **50**, 97–109.

Bover-Arnal, T., Salas, R., Moreno-Bedmar, J.A., Bitzer, K., 2009. Sequence stratigraphy and architecture of a late Early-Middle Aptian carbonate platform succession from the western Maestrat Basin (Iberian Chain, Spain). Sedimentary Geology **219**, 280–301.

Bover-Arnal, T., Moreno-Bedmar, J.A., Salas, R., Skelton, P.W., Bitzer, K., Gili, E., 2010. Sedimentary evolution of an Aptian syn-rift carbonate system (Maestrat Basin, E Spain): effects of accommodation and environmental change. Geologica Acta **8**, 249–280.

Bover-Arnal, T., Salas, R., Skelton, P.W., Gili, E., Moreno-Bedmar, J.A., 2011a. The Aptian carbonate platforms of the western Maestrat Basin: a textbook example of four systems tract-based sequence stratigraphy. In: Arenas, C., Pomar, L., Colombo, F. (Eds.), Pre-Meeting Field trips Guidebook, 28th IAS Meeting, Zaragoza. Sociedad Geológica de España, Geo-Guías **7**, 27–64.

Bover-Arnal, T., Salas, R., Martín-Closas, C., Schlagintweit, F., Moreno-Bedmar, J.A., 2011b. Expression of an oceanic anoxic event in a neritic setting: Lower Aptian coral rubble deposits from the western Maestrat Basin (Iberian Chain, Spain). Palaios **26**, 18–32.

Bover-Arnal, T., Löser, H., Moreno-Bedmar, J.A., Salas, R., Strasser, A., 2012. Corals on the slope (Aptian, Maestrat Basin, Spain). Cretaceous Research **37**, 43–64.

Bover-Arnal, T., Salas, R., Guimerà, J., Moreno-Bedmar, J.A., 2014. Deep incision on an Aptian carbonate succession indicates major sea-level fall in the Cretaceous. Sedimentology **61**, 1558–1593.

Bover-Arnal, T., Pascual-Cebrian, E., Skelton, P.W., Gili, E., Salas, R., 2015. Patterns in the distribution of Aptian rudists and corals within a sequence-stratigraphic framework (Maestrat Basin, E Spain). Sedimentary Geology **321**, 86–104.

Boulouard, C., Canérot, J., 1970. Données nouvelles sur l'Aptien supérieur et l'Albien dans le Bas-Aragón et le Maestrazgo (Espagne). Bulletin du Centre de Recherches Pau-SNPA **4**, 453–463.

Brand, U., Veizer, J., 1980. Chemical diagenesis of a multicomponent carbonate system: 1. Trace elements. Journal of Sedimentary Petrology **50**, 1219–1236.

Brand, U., Jiang, G., Azmy, K., Bishop, J., Montanez, I.P., 2012. Diagenetic evaluation of a Pennsylvanian carbonate succession (Bird Spring Formation, Arrow Canyon, Nevada, U.S.A) – 1:Brachiopod and whole rock comparison. Chemical Geology **308**, 26–39.

Brand, U., Logan, A., Bitner, M.A., Griesshaber, E., Azmy, K., Buhl, D., 2011. What is the ideal proxy of Paleozoic seawater chemistry? Memoirs of the Association of Australasian Palaeontologists **41**, 9–24.

Burla, S., Heimhofer, U., Hochuli, P.A., Weissert, H., Skelton, P., 2008. Changes in sedimentary patterns of coastal and deep-sea successions from the North Atlantic (Portugal) linked to Early Cretaceous environmental change: Palaeogeography, Palaeoclimatology, Palaeoecology **257**, 38–57.

Burla, S., Oberli, F., Heimhofer, U., Wiechert, U., Weissert, H., 2009. Improved time control on Cretaceous coastal deposits: new results from Sr isotope measurements using laser ablation. Terra Nova **21**, 401–409.

Caja, M.A., 2004. Procedencia y diagénesis de los sedimentos del Jurásico superior-Cretácico inferior (Facies Weald) en las subcuencas occidentales de la Cuenca del Maestrazgo, Cordillera Ibérica oriental. PhD thesis. Universidad Complutense de Madrid. 293 p.

Canérot, J., Cugny, P., Pardo, G., Salas, R., Villena, J., 1982. Ibérica Central-Maestrazgo. In: García, A. (Ed.), El Cretácico de España. Universidad Complutense de Madrid, 273–344.

Canudo, J.I., Royo-Torres, R., Cuenca-Bescós, G., 2008a. A new sauropod: Tastavinsaurus sanzi gen. et sp. nov. from the Early Cretaceous (Aptian) of Spain. Journal of Vertebrate Paleontology **28**, 712–731.

Canudo, J.I., Gasulla, J.M., Gómez-Fernández, D., Ortega, F., Sanz, J.L., Yagüe, P., 2008b. Primera evidencia de dientes aislados atribuidos a Spinosauridae (Theropoda) en el Aptiano inferior (Cretácico Inferior) de Europa: Formación Arcillas de Morella (España). Ameghiniana (Rev. Asoc. Paleontol. Argent.) **45**, 649–662.

Catuneanu, O., Abreu, V., Bhattacharya, J.P., Blum, M.D., Dalrymple, R.W., Eriksson, P.G., Fielding, C.R., Fisher, W.L., Galloway, W.E., Gibling, M.R., Giles, K.A., Holbrook, J.M., Jordan, R., Kendall, C.G.St.C., Macurda, B., Martinsen, O.J., Miall, A.D., Neal, J.E., Nummedal, D., Pomar, L., Posamentier, H.W., Pratt, B.R., Sarg, J.F., Shanley, K.W., Steel, R.J., Strasser, A., Tucker, M.E., Winker, C., 2009. Towards the standardization of sequence stratigraphy. Earth-Science Reviews **92**, 1–33.

Catuneanu, O., Galloway, W.E., Kendall, C.G.St.C., Miall, A.D., Posamentier, H.W., Strasser, A., Tucker, M.E., 2011. Sequence stratigraphy: methodology and nomenclature. Newsletters on Stratigraphy **44**, 173–245.

Clariana, M.P.,1999. Estratigrafía y sedimentología de las Facies Urgon (Aptiense) en la Subcuenca de Las Parras (Provincia de Teruel). PhD thesis. Universidad de Zaragoza, 132 p.

Clariana, M. P., Meléndez, A., Soria, A. R., 2000. Los depósitos terrígenos de la base de la secuencia de depósito Aptiense superior. Subcuenca de las Parras (provincia de Teruel). Geogaceta **27**, 43–45.

Cors, J., Heimhofer, U., Adatte, T., Hochuli, P.A., Huck, S., Bover-Arnal, T., 2015. Spore-pollen assemblages show delayed terrestrial cooling in the aftermath of OAE 1a. Geological Magazine **152**, 632–647.

de Gea, G.A., Rodríguez-López, J.P., Meléndez, N., Soria, A.R., 2008. Bioestratigrafía de la Fm. Escucha a partir del estudio de foraminíferos planctónicos y nanofósiles en el sector de Alcaine, Teruel. Geogaceta **44**, 115–118.

Delanoy, G., Busnardo, R., Ropolo, P., Gonnet, R., Conte, G., Moullade, M., Masse, J.P., 1997. The “Pseudocrioceras beds” at La Bédoule (SE France) and the position of the

Barremian-Aptian boundary in the historical lower Aptian stratotype. Compte Rendu de l'Académie des Sciences de Paris, Sciences de la Terre et des planètes **325**, 593–599.

Embry, J.-C., Vennin, E., Van Buchem, F. S. P., Schroeder, R., Pierre, C., Aurell, M., 2010. Sequence stratigraphy and carbon isotope stratigraphy of an Aptian mixed carbonate-siliciclastic platform to basin transition (Galve sub-basin, NE Spain). In: Van Buchem, F. S. P., Gerdes, K. D., Esteban, M. (Eds.), Mesozoic and Cenozoic Carbonate Systems of the Mediterranean and the Middle East: Stratigraphic and Diagenetic Reference Models. Geological Society Special Publications, London **329**, 113–143.

Föllmi, K.B., Weissert, H., Bisping, M., Funk, H., 1994. Phosphogenesis, carbon-isotope stratigraphy, and carbonate-platform evolution along the Lower Cretaceous northern Tethyan margin. Geological Society of America Bulletin **106**, 729–746.

Frijia, G., Parente, M., 2008. Strontium isotope stratigraphy in the upper Cenomanian shallow-water carbonates of the southern Apennines: short-term perturbations of marine $^{87}Sr/^{86}Sr$ during the oceanic anoxic event 2. Palaeogeography, Palaeoclimatology, Palaeoecology **261**, 15–29.

Frijia, G., Parente, M., Di Lucia, M., Mutti, M., 2015. Carbon and strontium isotope stratigraphy of the Upper Cretaceous (Cenomanian-Campanian) shallow-water carbonates of southern Italy: Chronostratigraphic calibration of larger foraminifera biostratigraphy. Cretaceous Research **53**, 110–139.

Gàmez, D., Paciotti, P., Colombo, F., Salas, R., 2003. La Formación Arcillas de Morella (Aptiense inferior), Cadena Ibérica oriental (España): caracterización sedimentológica. Geogaceta **34**, 191-194.

Garcia, R., Moreno-Bedmar, J.A., Bover-Arnal, T., Company, M., Salas, R., Latil, J.L., Martín-Martín, J.D., Gomez-Rivas, E., Bulot, L.G., Delanoy, G., Martínez, R., Grauges, A., 2014. Lower Cretaceous (Hauterivian-Albian) ammonite biostratigraphy in the Maestrat Basin (E Spain). Journal of Iberian Geology **40**, 99–112.

García-Mondéjar, J., Owen, H.G., Raisossadat, N., Millán, M.I., Fernández-Mendiola, P.A., 2009. The Early Aptian of Aralar (northern Spain): stratigraphy, sedimentology, ammonite biozonation, and OAE1. Cretaceous Research **30**, 434–464.

Gasulla, J.M., Ortega, F., Escaso, F., Pérez-García, A., 2011a. Los yacimientos de vertebrados de la Formación Arcillas de Morella (Aptiense inferior). In: Pérez-García, A., Gascó, F., Gasulla, J.M., Escaso, F. (Eds.), Viajando a Mundos Pretéritos. Ayuntamiento de Morella, Morella, Castellón, 157–172.

Gasulla, J.M., Ortega, F., Pereda-Suberbiola, X., Escaso, F., Sanz, J.L., 2011b. Elementos de la armadura dérmica del dinosaurio anquilosaurio Polacanthus Owen, 1865, en el Cretácico Inferior de Morella (Castellón, España). Ameghiniana **48**, 508–519.

Gasulla, J.M., Ortega, F., Sanz, J.L., Escaso, F., Yagüe, P., Pérez-García, A., 2012. Els vertebrats de la Formació Argiles de Morella (Aptià inferior, Cretaci Inferior). Nemus **2**, 15–27.

Gomez-Rivas, E., Corbella, M., Martín-Martín, J.D., Stafford, S.L., Teixell, A., Bons, P.D., Griera, A., Cardellach, E., 2014. Reactivity of dolomitizing fluids and Mg source evaluation of fault-controlled dolomitization at the Benicàssim outcrop analogue (Maestrat Basin, Spain). Marine and Petroleum Geology **55**, 26–42.

Gradstein, F.M., Ogg, J.G., Smith, A.G., 2004. A Geologic Time Scale 2004. Cambridge University Press, Cambridge, 610 p.

Hardenbol, J., Thierry, J., Farley, M.B., Jacquin, T., Graciansky, de P.-C., Vail, P.R., 1998. Mesozoic and Cenozoic sequence chronostratigraphic framework of European basins. In: Graciansky, de P.-C., Hardenbol, J., Jacquin, T., Vail, P.R. (Eds.), Mesozoic and Cenozoic sequence stratigraphy of European basins, SEPM Special Publication **60**, 3–13.

Hfaiedh, R., Arnaud Vanneau, A., Godet, A., Arnaud, H., Zghal, I., Ouali, J., Latil, J.-L., Jallali, H., 2013. Biostratigraphy and palaeoenvironmental evolution of the Aptian succession at Jebel Bir Oum Ali (Northern Chain of Chotts, South Tunisia). Cretaceous Research **46**, 177–207.

Huck, S., Heimhofer, U., Rameil, N., Bodin, S., Immenhauser, A., 2011. Strontium and carbon-isotope chronostratigraphy of Barremian-Aptian shoal-water carbonates: Northern Tethyan platform drowning predates OAE 1a. Earth and Planetary Science Letters **304**, 547–558.

Huck, S., Heimhofer, U., Immenhauser, A., Weissert, H., 2013. Carbon-isotope stratigraphy of Early Cretaceous (Urgonian) shoal-water deposits: Diachronous changes in carbonate-platform production in the north-western Tethys. Sedimentary Geology **290**, 157–174.

Husinec, A., Velic, I., Fucek, L., Vlahovic, I., Maticec, D., Ostric, N., Korbar, T., 2000. Mid Cretaceous orbitolinid (Foraminiferida) record from the islands of Cres and Losinj (Croatia) and its regional stratigraphic correlation. Cretaceous Research **21**, 155–171.

Husinec, A., Jelaska, V., 2006. Relative sea-level changes recorded on an isolated carbonate platform: Tithonian to Cenomanian succession, Southern Croatia. Journal of Sedimentary Research **76**, 1120–1136.

Jaramillo-Vogel, D., Strasser, A., Frijia, G., Spezzaferri, S., 2013. Neritic isotope and sedimentary records of the Eocene-Oligocene greenhouse-icehouse transition: The Calcare di Nago Formation (northern Italy) in a global context. Palaeogeography, Palaeoclimatology, Palaeoecology **369**, 361–376.

Jorquera-Grau, A., Santos-Cubedo, A., de Santisteban Bové, C., Galobart Lorente, A., 2009. Plesiosaurs (Reptilia: *Sauropterygia*) from the Arcillas de Morella Formation (Aptian, Lower Cretaceous) of Castellón (Spain). Paleolusitana **1**, 229–235.

Leonide, P., Borgomano, J., Masse, J-P., Doublet, S., 2012. Relation between stratigraphic architecture and multi-scale heterogeneities in carbonate platforms: The Barremian–lower Aptian of the Monts de Vaucluse, SE France. Sedimentary Geology **265**, 87–109.

López Llorens, J., 2007. Hallazgo de Imerites *giraudi giraudi*, ammonítido barremiense, en las "Arcillas de Morella". Consecuencias. Batalleria **13**, 53–56.

Marin, P., Sornay, J., 1971. Précisions sur l'âge des formations aptiennes aux confins de l'Aragón et du Maestrazgo (Provinces de Teruel et Castellón de la Plana, Espagne). Comptes Rendus sommaires de la Société géologique de France **3**, 165–167.

Martín-Martín, J.D., Gomez-Rivas, E., Bover-Arnal, T., Travé, A., Salas, R., Moreno-Bedmar, J.A., Tomás, S., Corbella, M., Teixell, A., Vergés, J., Stafford, S.L., 2013. The Upper Aptian to Lower Albian synrift carbonate succession of the southern Maestrat Basin (Spain): Facies architecture and fault-controlled stratabound dolostones. Cretaceous Research **41**, 217–236.

Martín-Martín, J.D., Travé, A., Gomez-Rivas, E., Salas, R., Sizun, J.-P., Vergés, J., Corbella, M., Stafford, S.L., Alfonso, P., 2015. Fault-controlled and stratabound dolostones in the Late Aptian-earliest Albian Benassal Formation (Maestrat Basin; E Spain): Petrology and geochemistry constraints. Marine and Petroleum Geology **66**, 83–102.

Martínez, R., Grauges, A., Salas, R., 1994. Distribución de los ammonites del Cretácico inferior de la Cordillera Costera Catalana e Ibérica Oriental. Cuadernos de Geología Ibérica **18**, 337–354.

Masse, J.-P., Fenerci-Masse, M., 2011. Drowning discontinuities and stratigraphic correlation in platform carbonates. The late Barremian-early Aptian record of southeast France. Cretaceous Research **32**, 659–684.

McArthur, J.M., Howarth, R.J., 2004. Strontium isotope stratigraphy. In: Gradstein, F., Ogg, J., Smith, A. (Eds.), A Geological Time Scale. Cambridge University Press, Cambridge, U.K, 96–105.

McArthur, J.M., Howarth, R.J., Bailey, T.R., 2001. Strontium isotope stratigraphy: lowess version 3. Best-fit to the marine Sr-isotope curve for 0 to 509 Ma and accompanying look-up table for deriving numerical age. Journal of Geology **109**, 155–170.

McArthur, J.M., Howarth, R.J., Shields, G.A., 2012. Strontium isotope stratigraphy. In: Gradstein, F.M., Ogg, J.G., Schmitz, M., Ogg, G. (Eds.), The Geologic Time Scale 2012. Elsevier Science Limited. 1144 p.

McArthur, J.M., 1994. Recent trends in strontium isotope stratigraphy. Terra Nova **6**, 331–358.

McArthur, J.M., Rio, D., Massari, F., Castratori, D., Bailey, T.R., Thirlwall, M., Houghton, S., 2006. A revised Pliocene record formarine $^{87}Sr/^{86}Sr$ used to date an interglacial event recorded in the Cockburn Island Formation, Antarctic Peninsula. Palaeogeography, Palaeoclimatology, Palaeoecology **242**, 126–136.

Menegatti, A.P., Weissert, H., Brown, R.S., Tyson, R.V., Farrimond, P., Strasser, A., Caron, M., 1998. High-resolution $\delta^{13}C$ stratigraphy through the early Aptian "Livello Selli" of the Alpine Tethys. Paleoceanography **13**, 530–545.

Moreno-Bedmar, J.A., Company, M., Bover-Arnal, T., Salas, R., Delanoy, G., Martínez, R., Grauges, A., 2009a. Biostratigraphic characterization by means of ammonoids of the lower Aptian Oceanic Anoxic Event (OAE1a) in the eastern Iberian Chain (Maestrat Basin, eastern Spain). Cretaceous Research **30**, 864–872.

Moreno-Bedmar, J.A., Company, M., Bover-Arnal, T., Salas, R., Maurrasse, F.J., Delanoy, G., Grauges, A., Martínez, R., 2010a. Lower Aptian ammonite biostratigraphy in the Maestrat Basin (Eastern Iberian Chain, Eastern Spain). A Tethyan transgressive record enhanced by synrift subsidence. Geologica Acta **8**, 281–299.

Moreno-Bedmar, J.A., Bover-Arnal, T., Barragán, R., Salas, R., 2012. Uppermost Lower Aptian transgressive records in Mexico and Spain: chronostratigraphic implications for the Tethyan sequences. Terra Nova **24**, 333–338.

Moreno-Bedmar, J.A., Bulot, L., Latil, J.L., Martínez, R., Ferrer, O., Bover-Arnal, T., Salas, R., 2008. Precisiones sobre la edad de la base de la Fm. Escucha, mediante ammonoideos, en la subcuenca de la Salzedella, Cuenca del Maestrat (E Cordillera Ibérica). Geo-Temas **10**, 1269–1272.

Moreno-Bedmar, J.A., Company, M., Barragán, R., Salas, R., Martín- Martín, J.D., Bover-Arnal, T., Gomez-Rivas, E., 2009b. Precisiones, mediante ammonoideos, sobre la edad de la Fm. Benassal, Cuenca del Maestrat (Cadena Ibérica). In: Palmqvist, P., Pérez-Claros, J.A. (Coords.), XXV Jornadas de la Sociedad Española de Paleontología. Libro de Resúmenes. Universidad de Málaga, 231–234.

Moreno-Bedmar, J.A., 2010. Ammonits de l'Aptià inferior de la península Ibèrica. Biostratigrafia i aportacions a l'estudi del Oceanic Anoxic Event 1a. PhD thesis, Universitat de Barcelona, Barcelona, 331 p.

Moreno-Bedmar, J.A., Garcia, R., Salas, R., Ferrer, O., 2010b. Bioestratigrafía de los ammonites del Aptiense inferior (Cretácico Inferior) del Perelló (Tarragona). In: Moreno-Azanza, M., Díaz-Martínez, I., Gasca, J.M., Melero-Rubio, M., Rabal-Garcés, R., Sauqué, V. (Eds.). VIII Encuentro de Jóvenes Investigadores en Paleontología, volumen de actas, Cidaris **30**, 201–204.

Moreno-Bedmar, J.A., Garcia, R., 2011. Análisis bioestratigráfico de los ammonoideos del Aptiense inferior (Cretácico Inferior) del Miembro Cap de Vinyet (Formación Margas del Forcall) de la subcuenca de Morella (Castellón). Consideraciones sobre el límite Barremiense-Aptiense. In: Pérez-García, A., Gascó, F., Gasulla, J.M., Escaso, F. (Eds.), Viajando a Mundos Pretéritos. Ayuntamiento de Morella, Morella, Castellón, 215–222.

Moreno-Bedmar, J.A., Barragán, R., Delanoy, G., Company, M., Salas, R., 2014. Review of the early Aptian (Early Cretaceous) ammonoid species *Deshayesites deshayesi* (d'Orbigny, 1841). Cretaceous Research **51**, 341–360.

Moullade, M., Tronchetti, G., Granier, B., Bornemann, A., Kuhnt, W., Lorenzen; J., 2015. High-resolution integrated stratigraphy of the OAE1a and enclosing strata from core drillings in the Bedoulian stratotype (Roquefort-La Bédoule, SE France). Cretaceous Research **56**, 119–140.

Murat, B., 1983. Contribution à l'étude stratigraphique, sedimentologique et tectonique du bassin éocrétace d'Oliete (Prov. de Teruel, Espagne). PhD thesis, Université Paul Sabatier, Tolouse, 247 p.

Mutterlose, J., Bodin, S., Fähnrich, L., 2014. Strontium-isotope stratigraphy of the Early Cretaceous (Valanginian–Barremian): Implications for Boreal–Tethys correlation and paleoclimate. Cretaceous Research **50**, 252–263.

Pardo, G., 1979. Estratigrafía y sedimentología de las formaciones detríticas del Cretácico inferior terminal del Bajo Aragón Turolense. PhD thesis, Universidad de Zaragoza, 473 p.

Pardo, G., Villena, J., 1979. Características sedimentológicas y paleogeográficas de la Fm. Escucha. Cuadernos de Geología Ibérica **5**, 407–418.

Pascual-Cebrian, E., 2014. Shell evolution of the Polyconitidae during the Aptian of Iberia: A grinding tomography method to map calcite/aragonite fluctuations in rudist bivalves. PhD thesis, Universität Heidelberg, 144 p.

Pérez-García, A., Ortega, F., Gasulla, J.M., 2009. Revisión histórica y sistemática del primer hallazgo de tetanuros basales (Theropoda) del Cretácico Inferior de Morella (Castellón). Geogaceta **47**, 21–24.

Pérez-García, A., Gasulla, J.M., Ortega, F., 2014. *Eodortoka morellana* gen. et sp. nov., the first pan-pleurodiran turtle (Dortokidae) defined in the Lower Cretaceous of Europe. Cretaceous Research **48**, 130–138.

Peropadre, C., 2012. El Aptiense del margen occidental de la cuenca del Maestrazgo: controles tectónico, eustático y climático en la sedimentación. PhD thesis, Universidad Complutense de Madrid, 649 p.

Peyrot, D., Rodríguez-López, J.P., Barrón, E., Meléndez, N., 2007. Palynology and biostratigraphy of the Escucha Formation in the Early Cretaceous Oliete sub-basin, Teruel, Spain. Revista Española de Micropaleontología **39**, 135–154.

Pictet, A., Delanoy, G., Adatte, T., Spangenberg, J.E., Baudouin, C., Boselli, P., Boselli, M., Kindler, P., Föllmi, K.B., 2015. Three successive phases of platform demise during the early Aptian and their association with the oceanic anoxic Selli episode (Ardèche, France). Palaeogeography, Palaeoclimatology, Palaeoecology **418**, 101–125.

Querol, X., 1990. Distribución de la materia mineral y azufre en los carbones de la Fm. Escucha. Relación con los factores geológicos, sedimentológicos y diagenéticos. PhD thesis, Universitat de Barcelona, 509 p.

Querol, X., Salas, R., Pardo, G., Ardèvol, L., 1992. Albian coal-bearing deposits of the Iberian Range in northeastern Spain. In: McCabe, P.J., Parrish, J.T. (Eds.), Controls on the distribution and quality of Cretaceous coals. Geological Society of America Special Paper **267**, 193–208.

Reboulet, S., Rawson, P.F., Moreno-Bedmar, J.A., Aguirre-Urreta, M.B., Barragán, R., Bogomolov, Y., Company, M., González-Arreola, C., Stoyanova, V.I., Lukeneder, A., Matrion, B., Mitta, V., Randrianaly, H., Vasicek, Z., Baraboshkin, E.J., Bert, D., Bersac, S., Bogdanova, T.N., Bulot, L.G., Latil, J.-L., Mikhailova, I.A., Ropolo, P., Szives, O., 2011. Report on the 4th International Meeting of the IUGS Lower Cretaceous Ammonite Working Group, the “Kilian Group” (Dijon, France, 30th August 2010). Cretaceous Research **32**, 786–793.

Reboulet, S., Szives, O., Aguirre-Urreta, B., Barragán, R., Company, M., Idakieva, V., Ivanov, M., Kakabadze, M.V., Moreno-Bedmar, J.A., Sandoval, J., Baraboshkin, E.J., Çaglar, M.K., Főzy, I., González-Arreola, C., Kenjo, S., Lukeneder, A., Raisossadat, S.N., Rawson, P.F., Tavera, J.M., 2014. Report on the 5th International Meeting of the IUGS Lower Cretaceous Ammonite Working Group, the Kilian Group (Ankara, Turkey, 31st August 2013). Cretaceous Research **50**, 126–137.

Ropolo, P., Gonnet, R., Conte, G., 1999. The “*Pseudocrioceras* interval” and adjacent beds at La Bédoule (SE France): implications to highest Barremian/lowest Aptian biostratigraphy. Scripta Geologica, Special Issue **3**, 159–213.

Ropolo, P., Conte, G., Gonnet, R., Masse, J.-P., Moullade, M., 2000. Les faunes d’Ammonites du Barrémien supérieur/Aptien inférieur (Bédoulien) dans la région stratotypique de Cassis-La Bédoule (SE France): état des connaissances et propositions pour une zonation par Ammonites du Bédoulien-type. Géologie Méditerranéenne **25**, 167–175.

Sahagian, D., Pinous, O., Olferiev, A., Zakharov, V., 1996. Eustatic curve for the Middle Jurassic-Cretaceous based on Russian Platform and Siberian stratigraphy: zonal resolution. AAPG Bulletin **80**, 1433–1458.

Salas, R., 1987. El Malm i el Cretaci inferior entre el Massís de Garraf i la Serra d'Espadà. Anàlisi de Conca. PhD thesis, Universitat de Barcelona, 345 p.

Salas, R., Guimerà, J., Mas, R., Martín-Closas, C., Meléndez, A., Alonso, A., 2001. Evolution of the Mesozoic Central Iberian Rift System and its Cainozoic inversion (Iberian Chain). In: Ziegler, P.A., Cavazza, W., Roberston, A.H.F., Crasquin-Soleau, S. (Eds.), Peri-Tethys Memoir 6: Peri-Tethyan Rift/Wrench Basins and Passive Margins. Mémoires du Muséum National d'Histoire Naturelle, Paris **186**, 145–186.

Salas, R., Casas, A., 1993. Mesozoic extensional tectonics, stratigraphy, and crustal evolution during the Alpine cycle of the eastern Iberian basin. Tectonophysics **228**, 33–55.

Salas, R., Martín-Closas, C., Querol, X., Guimerà, J., Roca, E., 1995. In: Salas, R., Martín-Closas, C. (Eds.), El Cretácico inferior del nordeste de Iberia. Publicacions de la Universitat de Barcelona, 13–94.

Salas, R., Guimerà, J., 1996. Rasgos estructurales principales de la cuenca Cretácica Inferior del Maestrazgo (Cordillera Ibérica oriental). Geogaceta **20**, 1704–1706.

Schlagintweit, F., Bover-Arnal, T., Salas, R., 2010. Erratum to: New insights into *Lithocodium aggregatum* Elliott 1956 and *Bacinella irregularis* Radoičić 1959 (Late Jurassic-Lower Cretaceous): two ulvophycean green algae (?Order Ulotrichales) with a heteromorphic life cycle (epilithic/euendolithic). Facies **56**, 635–673.

Schlagintweit, F., Bover-Arnal, T., 2012. The morphological adaption of *Lithocodium aggregatum* Elliott (calcareous green alga) to cryptic microhabitats (Lower Aptian, Spain): an example of phenotypic plasticity. Facies **58**, 37–55

Schlagintweit, F., Bover-Arnal, T., 2013. Remarks on *Bacinella* Radoicic, 1959 (type species *B. irregularis*) and its representatives. Facies **59**, 59–73

Schroeder, R., van Buchem, F.S.P., Cherchi, A., Baghbani, D., Vincent, B., Immenhauser, A., Granier, B., 2010. Revised orbitolinid biostratigraphic zonation for the Barremian – Aptian of the eastern Arabian Plate and implications for regional stratigraphic correlations. In: van Buchem, F.S.P., Al-Husseini, M.I., Maurer, F., Droste, H.J. (Eds.), Barremian – Aptian Stratigraphy and Hydrocarbon Habitat of the Eastern Arabian Plate. GeoArabia Special Publication 4, Gulf PetroLink, Bahrain **1**, 49–96.

Schroeder, R., 1964. Orbitoliniden-biostratigraphie des Urgons nordöslich von Teruel (Spanien). Neues Jahrbuch für Geologie und Paläontologie. Monatshefte **8**, 462–474.

Skelton, P.W., Gili, E., 2012. Rudists and carbonate platforms in the Aptian: a case study on biotic interactions with ocean chemistry and climate. Sedimentology **59**, 81–117.

Skelton, P.W., Gili, E., Bover-Arnal, T., Salas, R., Moreno-Bedmar, J.A., 2010. A new species of *Polyconites* from the uppermost Lower Aptian of Iberia and the early evolution of polyconitid rudists. Turkish Journal of Earth Sciences **19**, 557–572.

Solé de Porta, N., Salas, R., 1994. Conjuntos microflorísticos del Cretácico inferior de la Cuenca del Maestrazgo. Cordillera Ibérica Oriental (NE de España). Cuadernos de Geología Ibérica **18**, 355–368.

Solé de Porta, N., Querol, X., Cabanes, R., Salas, R., 1994. Nuevas aportaciones a la palinología y paleoclimatología de la Formación Escucha (Albiense inferior-medio) en las Cubetas de Utrillas y Oliete. Cordillera Ibérica Oriental. Cuadernos de Geología Ibérica **18**, 203–215.

Sornay, J., Marin, P., 1972. Sur la faune d'ammonites aptiennes de la Tejeria de Josa (Teruel, Espagne). Annales de Paléontologie (Invertébrés), t. LVIII, 101–114.

Suarez-Gonzalez, P., Quijada, I.E., Benito, M.I., Mas, R., 2013. Eustatic versus tectonic control in an intraplate rift basin (Leza Fm, Cameros Basin). Chronostratigraphic and paleogeographic implications for the Aptian of Iberia. Journal of Iberian Geology **39**, 285–312.

Stein, M., Arnaud-Vanneau, A., Adatte, T., Fleitmann, D., Spangenberg, J.E. and Föllmi, K.B., 2012. Palaeoenvironmental and palaeoecological change on the northern Tethyan carbonate platform during the Late Barremian to earliest Aptian. Sedimentology **59**, 939–963.

Steuber, T., 1999. Isotopic and chemical intra-shell variations in low-Mg calcite of rudist bivalves (Mollusca: Hippuritacea): disequilibrium fractionations and Late Cretaceous seasonality. International Journal Earth Sciences **88**, 551–570.

Steuber, T., 2001. Strontium isotope stratigraphy of TuronianeCampanian Gosau-type rudist formations in the Northern Calcareous and Central Alps (Austria and Germany). Cretaceous Research **22**, 429–441.

Steuber, T., 2003a. Strontium isotope chemostratigraphy of rudist bivalves and cretaceous carbonate platforms. In: Gili, E., Negra, M.E.H., Skelton, P.W. (Eds.), North African Cretaceous Carbonate Platform Systems, NATO Science Series, IV. Earth and Environmental Sciences **28**, 229–238.

Steuber, T., 2003b. Strontium isotope stratigraphy of Cretaceous hippuritid rudist bivalves: rates of morphological change and heterochronic evolution. Palaeogeography, Palaeoclimatology, Palaeoecology **200**, 221–243.

Steuber, T., Schlüter, M., 2012. Strontium-isotope stratigraphy of Upper Cretaceous rudist bivalves: biozones, evolutionary patterns and sea-level change calibrated to numerical ages. Earth-Science Reviews **114**, 42–60.

Steuber, T., Korbar, T., Jelaska, V., Gusic, I., 2005. Strontium isotope stratigraphy of Upper Cretaceous platform carbonates of the island of Brac (Adriatic Sea, Croatia): implications for global correlation of platform evolution and biostratigraphy. Cretaceous Research **26**, 741–756.

Tomás, S., Löser, H., Salas, R., 2008. Low-light and nutrient-rich coral assemblages in an Upper Aptian carbonate platform of the southern Maestrat Basin (Iberian Chain, eastern Spain). Cretaceous Research **29**, 509–534.

Vail, P.R., Audemard, F., Bowman, S.A., Eisner, P.N., Perez-Cruz, C., 1991. The stratigraphic signatures of tectonics, eustasy and sedimentology - an overview. In: Einsele, G., Ricken, W., Seilacher, A. (Eds.), Cycles and Events in Stratigraphy, Springer, Berlin, 617–659.

Vennin, E., Aurell, M., 2001. Stratigraphie sequentielle de l'Aptien du sous-basin de Galvé (Province de Teruel, NE de l'Espagne). Bulletin de la Société Géologique de France **172**, 397–410.

Vicedo, V., Frijia, G., Parente, M., Caus, E., 2011. The late Cretaceous genera *Cuvillierinella*, *Cyclopseudedomia* and *Rhapydionina* (Rhapydioninidae, Foraminiferida) in shallow water carbonates of Pylos (Peloponnese, Greece). Journal of Foraminiferal Research **41**, 41–52.

Vilas, L., Masse, J.P., Arias, C., 1995. *Orbitolina* episodes in carbonate platform evolution: the early Aptian model from SE Spain. Palaeogeography, Palaeoclimatology, Palaeoecology, **119**, 35–45.

Villanueva-Amadoz, U., Pons, D., Diez, J. B., Ferrer, J., Sender, L.M., 2010. Angiosperm pollen grains of Sant Just site (Escucha Formation) from the Albian of the Iberian Range (north-eastern Spain). Review of Palaeobotany and Palynology **162**, 362–381.

Villanueva-Amadoz, U., Santisteban, C., Santos-Cubedo, A., 2014. Age determination of the Arcillas de Morella Formation (Maestrazgo Basin, Spain), Historical Biology **27**, 389–397.

Wagreich, M., Hohenegger, J., Neuhuber, S., 2012. Nannofossil biostratigraphy, strontium and carbon isotope stratigraphy, cyclostratigraphy and an astronomically calibrated duration of the Late Campanian *Radotruncana calcarata* Zone. Cretaceous Research **38**, 80–96.

Weisser, D., 1959. Acerca de la estratigrafía del Urgo-Aptense en las cadenas Celtibericas de España. Notas y Comunicaciones del Instituto Geológico y Minero de España **55**, 17–32.

Williamson, T., Henderson, R.A., Price, G.D., Collerson, K.D., 2012. Strontium–isotope stratigraphy of the Lower Cretaceous of Australia. Cretaceous Research **36**, 24–36.

Wissler, L., Funk, H., Weissert, H., 2003. Response of Early Cretaceous carbonate platforms to chages in atmospheric carbon dioxide levels. Palaeogeography, Palaeoclimatology, Palaeoecology **200**, 187–205.

Yagüe, P., Ortega, F., Noé, L.F., Gasulla, J.M., García, M.D., 2003. Reptiles marinos (Plesiosauria) del Aptiense inferior de Morella (Castellón). In: Perez-Lorente, F. (Coord.), Dinosaurios y otros reptiles mesozoicos de España. Ciencias de la Tierra, Logroño **26**, 399–404.

Zalasiewicz, J., Smith, A., Brenchley, P., Evans, J., Knox, R., Riley, N., Gale, A., Gregory, F.J., Rushton, A., Gibbard, P., Hesselbo, S., Marshall, J., Oates, M., Rawson, P., Trewin, N., 2004. Simplifying the stratigraphy of time. Geology **32**, 1–4.

Figures

Figure 1. A) Map of the Iberian Peninsula with the situation of the Maestrat Basin in the eastern part of the Iberian Chain. B) Schematic palaeogeographical map of the Maestrat Basin during the Late Jurassic-Early Cretaceous extensional period subdivided into its seven sub-basins, namely Oliete (Ol), Aliaga (Al), Galve (Ga), Penyagolosa (Pg), Morella (Mo), El Perelló (Pe) and Salzedella (Sa). Modified after Salas et al. (2001). Sampling locations for Sr-isotope stratigraphy are marked with a circle. See Fig. 4 for key. The location of the ammonite *Martelites* sp. found during the writing of this study is marked with a red star.

Figure 2. Litho-stratigraphic framework of the Late Barremian-Early Aptian sedimentary record of the Maestrat Basin showing the classical (black arrows A1-A2) and this study's (black arrow B) stratigraphic positions of the Barremian-Aptian boundary. See Fig. 4 for key.

Figure 3. Chrono-stratigraphic chart for the Barremian-Early Albian of the Maestrat Basin including the more relevant ammonoid, orbitolinid and rudist occurrences, Sr-derived numerical ages, major transgressive-regressive sequences and lithostratigraphic units. The ranges of the fossils are facies and stratigraphically constrained to their occurrences in the sections studied in the Maestrat Basin by Weisser (1959), Schroeder (1964), Aguilar et al. (1971), Marin and Sornay (1971), Sornay and Marin (1972), Canérot et al. (1982), Salas (1987), Martínez et al. (1994), López Llorens (2007), Moreno-Bedmar et al. (2008, 2009a, b, 2010a, b, 2012, 2014), Tomás et al. (2008), Bover-Arnal et al. (2009, 2010, 2011a, b, 2012, 2014, 2015), Moreno-Bedmar (2010), Schlagintweit et al. (2010), Skelton et al. (2010), Moreno-Bedmar and Garcia (2011), Peropadre (2012), Schlagintweit and Bover-Arnal (2012), Skelton and Gili (2012), Martín-Martín et al. (2013), Pascual-Cebrian (2014) and Garcia et al. (2014). Numerical ages, geo-magnetic polarity intervals and ammonite zones are taken from Gradstein et al. (2004). Barremian-Early Albian sequence-stratigraphic framework

of European basins is characterized in Hardenbol et al. (1998), and tied to numerical ages in Gradstein et al. (2004). The ammonite zones identified are dashed in grey. Different species and corresponding ranges are distinguished by using different colours. The Barremian Camarillas and Cantaperdius formations are outside the scope of this paper and are thus not detailed in the figure. The Camarillas Formation mainly consists of continental clastics, and the Cantaperdius Formation is formed by lacustrine limestones and marls. See Fig. 4 for key.

Figure 4. Key to Figure 3.

Figure 5. Lithostratigraphy and major transgressive-regressive cycles of the Late Barremian sedimentary record of the Maestrat Basin. A) Panoramic view of the Late Barremian Artoles, Morella and Xert lithostratigraphic units cropping out along the Barranco de las Calzadas section (see Bover-Arnal et al. 2010 for situation), 500 m to the west of the village of Miravete de la Sierra (*Comarca* of El Maestrazgo) in the Galve sub-basin (Fig. 1B). The first major transgressive-regressive sequence and the lowermost part of the transgressive unit of Sequence II are indicated. Note the reddish colour (continental record) mainly exhibited by the Morella Formation and the bluish colour (marine record) shown by the Artoles and Xert formations. Width of image is *c*. 280 m. See Fig. 4 for legend. B) Outcrop view of the Late Barremian Morella Formation. The transgressive-regressive sequence-stratigraphic interpretation is indicated. Note the reddish colour (continental record) of the succession below the sharp to slightly erosive transgressive surface (TS), and how above this surface the Morella Formation exhibits a bluish colour (marine record). The quarry pit where this photo was taken is located in the Morella sub-basin (Fig. 1B), 4 km to the southwest of the town of Morella (*Comarca* of Els Ports). Width of image is *c*. 60 m. See Fig. 4 for legend. C) Outcrop view of the Late Barremian transitional Cervera del Maestrat Formation. The abandoned

quarry pit where this photo was taken is located in the Salzedella sub-basin (Fig. 1B), 1.2 km to the northeast of the town of Cervera del Maestrat (*Comarca* of El Baix Maestrat). Width of image is *c*. 35 m.

Figure 6. Lithostratigraphy and major transgressive-regressive cycles of the Late Barremian-Late Aptian sedimentary record of the Maestrat Basin. A) Panoramic view of the Late Barremian-latest Aptian Penyagolosa section (see Salas 1987 and Salas et al. 1995 for situation) including the transgressive-regressive sequence-stratigraphic interpretation. This section, which gives rise to the Penyagolosa Massif, crops out 5 km to the northeast of the town of Villafermosa (*Comarca* of l'Alt Millars), in the Penyagolosa sub-basin (Fig. 1B). Width of image is *c*. 3.7 km. TS=Transgressive surface; MFS=Maximum flooding surface. See Fig. 4 for legend. B) Panoramic view of the Mola de Xert located 1.5 m to the north of the town of Xert (*Comarca* of El Baix Maestrat). The limestones of the Late Barremian Xert Formation and the marls and platform carbonates of the Early Aptian Forcall and Villarroya de los Pinares formations, respectively, can be easily recognized. The transgressive-regressive sequence stratigraphic interpretation is indicated. Width of image is *c*. 1.4 km. See Fig. 4 for legend. C) Outcrop view of Sequence II, which includes the Xert, Forcall and Villarroya de los Pinares formations, at the northern entrance to the town of Villarroya de los Pinares (*Comarca* of El Maestrazgo), in the Galve sub-basin (Fig. 1B). The transgressive-regressive sequence-stratigraphic interpretation is indicated. Width of image is *c*. 200 m. See Fig. 4 for legend.

Figure 7. Lithostratigraphy and major transgressive-regressive cycles of the Late Barremian-Late Aptian sedimentary record of the Maestrat Basin. A) Panoramic photo showing the latest Barremian-early Late Aptian lithostratigraphy of the Maestrat Basin including the Xert,

Forcall, Villarroya de los Pinares and Benassal (lower part) formations. The transgressive-regressive sequence-stratigraphic interpretation is indicated. This succession is exposed along the eastern limb of the Camarillas syncline, which is located to 3.5 km the northwest of the viallage of Miravete de la Sierra (*Comarca* of El Maestrazgo), in the Galve sub-basin (Fig. 1B). Width of image is *c*. 450 m. TS=Transgressive surface; MFS=Maximum flooding surface. See Fig. 4 for legend. B) Field view of the Early Aptian Forcall Formation cropping out in El Perelló sub-basin (Fig. 1B). The photo was taken along the highway A7 in a road cut located 2 km to the northeast of the town of El Perelló (*Comarca* of El Baix Ebre). Geologist at left for scale is 1.61 m tall without boots. C) Field view of sequences II and III including the Forcall, Villarroya de los Pinares and Benassal formations. The transgressive-regressive sequence-stratigraphic interpretation is indicated. This hillock (La Mola d'en Camaràs; see Bover-Arnal et al. 2014) is located 1.3 km to the northeast of the town of El Forcall (*Comarca* of Els Ports), in the Morella sub-basin (Fig. 1B). Width of image is *c*. 25 m. TS=Transgressive surface; MFS=Maximum flooding surface. See Fig. 4 for legend. D) Outcrop view of Sequence III, which corresponds to the lower part of the Benassal Formation. The transgressive-regressive sequence-stratigraphic interpretation is indicated. This outcrop is located in the Barranco de las Corralizas section (see Bover-Arnal et al. 2010 for situation; sample B2 was collected in this locality; Fig. 3 and Table 1), 2.4 km to the west of the village of Miravete de la Sierra (*Comarca* of El Maestrazgo), in the Galve sub-basin (Fig. 1B). Width of image is *c*. 350 m.

Figure 8. Lithostratigraphy and major transgressive-regressive cycles of the Late Aptian-Early Albian sedimentary record of the Maestrat Basin. A) Field view of the Benassal Formation, which gives rise to the Orpesa Range between the towns of Orpesa and Benicàssim (*Comarca* of La Plana Alta), in the Penyagolosa sub-basin (Fig. 1B). Width of

image is approximately 4 km. B) Field view of the three transgressive-regressive cycles (III, IV and V) of the Benassal Formation in the Barranco del Portolés section (see Vennin and Aurell 2001, Embry et al. 2010 and Bover-Arnal et al. 2010 for situation), located 1.3 km to the north of the town of Villarroya de los Pinares (*Comarca* of El Maestrazgo), in the Galve sub-basin (Fig. 1B). Width of image is *c*. 130 m. TS=Transgressive surface; MFS=Maximum flooding surface. See Fig. 4 for legend. C) Outcrop view of the Albian coal-bearing Escucha Formation in the environs of the town of Aliaga (*Comarca* of El Maestrazgo), in the Galve sub-basin (Fig. 1B). Transgressive unit of Sequence VI. Jacob's staff = 1.5 m.

Figure 9. *Martelites* sp. Lateral and ventral views of the specimen PUAB 90990 (=PUAB Collections of Paleontology of the Universitat Autònoma de Barcelona, Bellaterra, Spain), which was collected in the lower part of the Xert Formation cropping out in Torre Miró (km. 70 of the N-232 road), in the Morella sub-basin (Fig. 1B). The black arrow indicates the initial helically coiled whorls that are characteristic of the Family Heteroceratidae. The white triangles mark the last septa. Scale bar is 1 cm.

Table

Table 1. A) Analytical results of low-Mg calcite of rudist, oyster and brachiopod shells from the Maestrat Basin analysed for this study. See Fig. 1B for location of the samples collected. Numerical ages are derived from McArthur et al. (2001; look-up table version 4; 08/04). Numerical ages on the left side of the figure are taken from Gradstein et al. (2004). ±2 s.e. = 2 standard error. na = not applicable; P = Pristine; PA = Probably Altered; A = Altered. The analytical results written in italics were not used to derive numerical ages due to possible alteration of the sample. The analytical results used to calculate ages are written in bold. B)

Analytical results of low-Mg calcite of rudist shells from the western Maestrat Basin (Galve sub-basin; Fig. 1B) obtained by Pascual-Cebrian (2014). Numerical ages are derived from McArthur et al. (2001; look-up table version 4; 08/04). Numerical ages are taken from Gradstein et al. (2004). ±2 s.e. = 2 standard error. P = Pristine; PA = Probably Altered.

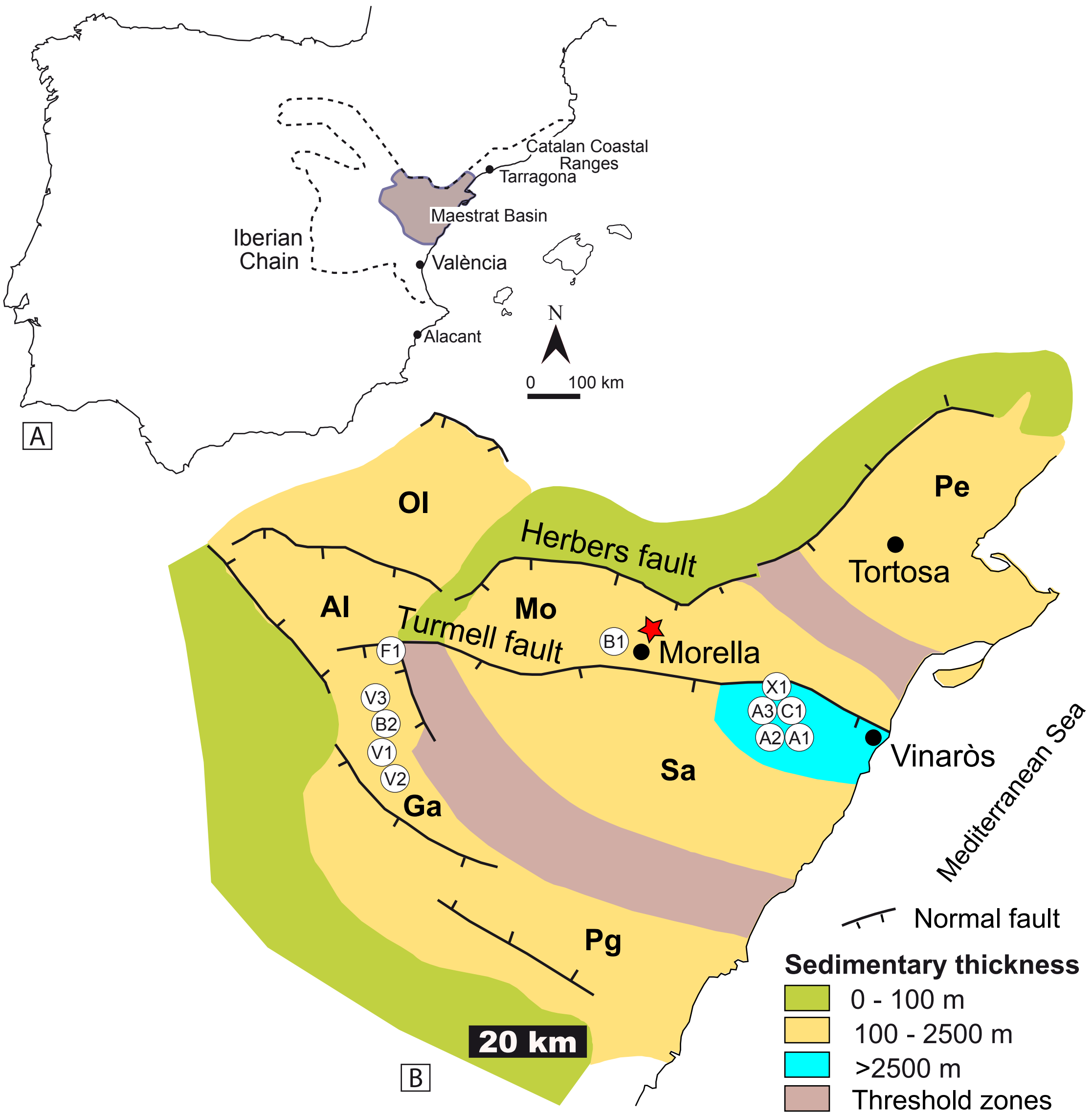

Catalan Coastal Ranges
Tarragona
Maestrat Basin
Iberian Chain
València
Alacant
N
0 100 km
A
Ol
Herbers fault
Pe
Tortosa
Al
Mo
Turmell fault
F1
B1
Morella
X1
A3
C1
A2
A1
V3
B2
V1
V2
Vinaròs
Ga
Sa
Mediterranean Sea
Pg
Normal fault
Sedimentary thickness
0 - 100 m
100 - 2500 m
>2500 m
Threshold zones
20 km
B

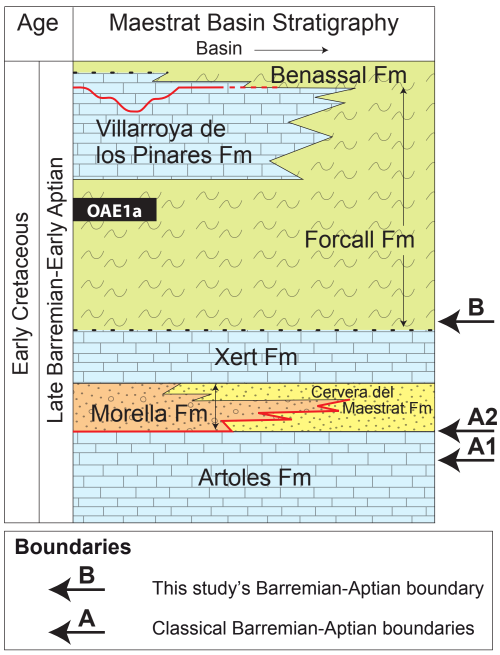
Age
Maestrat Basin Stratigraphy
Basin
Early Cretaceous
Late Barremian-Early Aptian
Benassal Fm
Villarroya de
los Pinares Fm
OAE1a
Forcall Fm
B
Xert Fm
Cervera del
Maestrat Fm
Morella Fm
A2
A1
Artoles Fm
Boundaries
B
This study's Barremian-Aptian boundary
A
Classical Barremian-Aptian boundaries

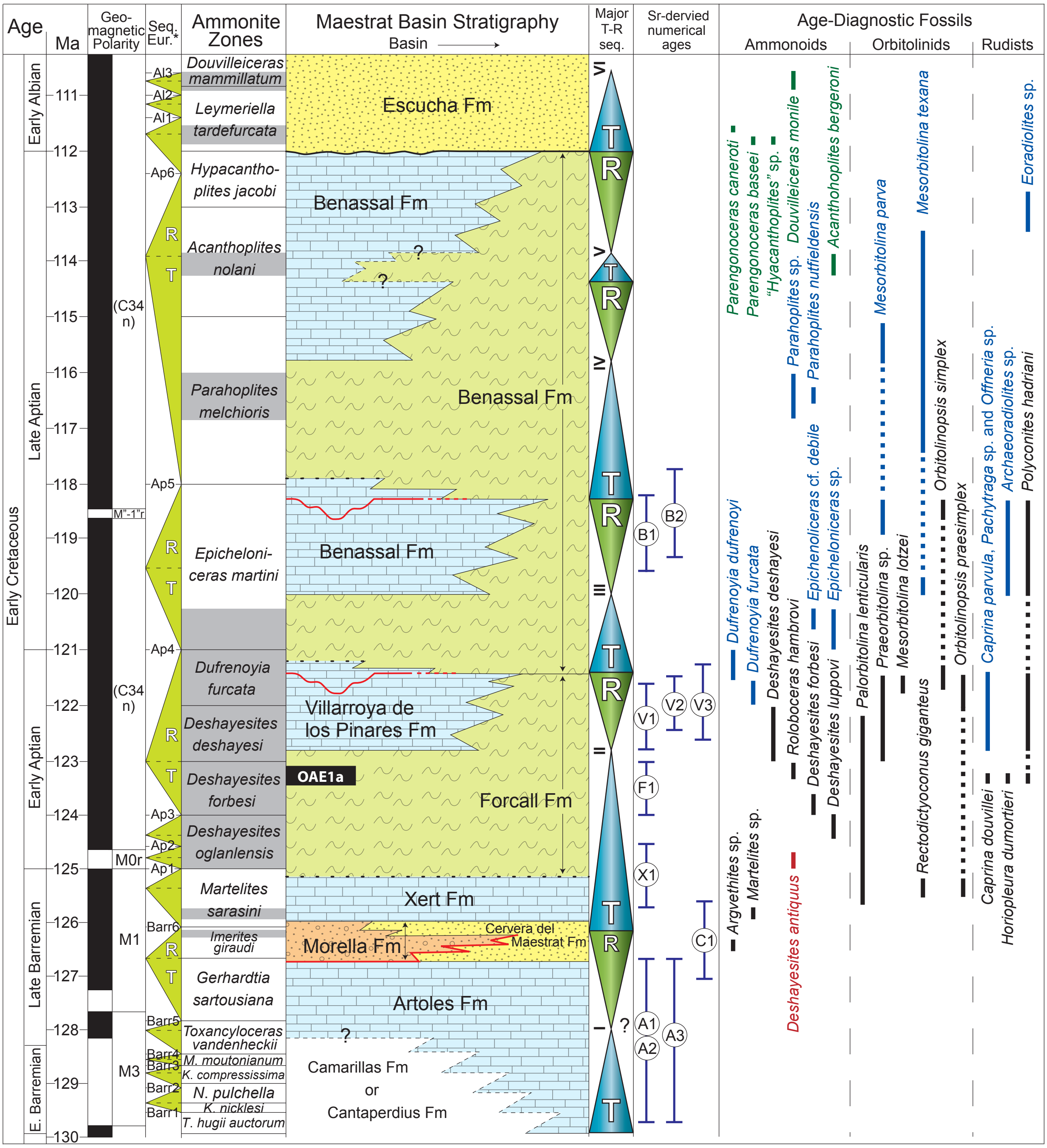

Age
Ma
Geo-magnetic Polarity
Seq. Eur.*
Ammonite Zones
Maestrat Basin Stratigraphy
Basin
Major T-R seq.
Sr-dervied numerical ages
Age-Diagnostic Fossils
Ammonids
Orbitolinids
Rudists
Early Cretaceous
Early Albian
Late Aptian
Early Aptian
Late Barremian
E. Barremian
(C34 n)
M"-1"r
M0r
M1
M3
Douvilleiceras mammillatum
Leymeriella tardefurcata
Hypacanthoplites jacobi
Acanthoplites nolani
Parahoplites melchioris
Epicheloniceras martini
Dufrenoyia furcata
Deshayesites deshayesi
Deshayesites forbesi
Deshayesites oglanlensis
Martelites sarasini
Imerites giraudi
Gerhardtia sartousiana
Toxancyloceras vandenheckii
M. moutonianum
K. compressissima
N. pulchella
K. nicklesi
T. hugii auctorum
Escucha Fm
Benassal Fm
Villarroya de los Pinares Fm
Forcall Fm
OAE1a
Xert Fm
Morella Fm
Cervera del Maestrat Fm
Artoles Fm
Camarillas Fm or Cantaperdius Fm
B1
B2
V1
V2
V3
F1
X1
C1
A1
A2
A3
Parengonoceras caneroti
Parengonoceras baseei
"Hyacanthoplites" sp.
Douvilleiceras monile
Parahoplites sp.
Parahoplites nutfieldensis
Acanthohoplites bergeroni
Dufrenoyia dufrenoyi
Dufrenoyia furcata
Deshayesites deshayesi
Roloboceras hambrovi
Epichenoliceras cf. debile
Deshayesites forbesi
Epicheloniceras sp.
Deshayesites luppovi
Argvethites sp.
Martelites sp.
Deshayesites antiquus
Mesorbitolina parva
Mesorbitolina texana
Palorbitolina lenticularis
Praeorbitolina sp.
Mesorbitolina lotzei
Rectodictyoconus giganteus
Orbitolinopsis simplex
Orbitolinopsis praesimplex
Caprina parvula, Pachytraga sp. and Offneria sp.
Archaeoradiolites sp.
Eoradiolites sp.
Polyconites hadriani
Caprina douvillei
Horiopleura dumortieri

Key

Basinal marine marls and limestones

Platform and transitional limestones, sandy limestones and marls

Continental clastics

Coastal and shallow-subtidal clastics

Correlative conformity

Eorsional unconformity

Surface of subaerial exposure

Lithostratiraphic boundary lacking absolute dating

Drowning surface

Deeply incised subaerial unconformity

T Transgressive

R Regressive

- (A1) Brachiopod shells, Artoles Formation, Corral d'en Parra, Salzedella sub-basin
- (A2) Oyster shells, Artoles Formation, Corral d'en Parra, Salzedella sub-basin
- (A3) Oyster shells, Artoles Formation, Mas del Regall, Salzedella sub-basin
- (C1) Oyster shells, Cervera del Maestre Formation, Mas del Regall, Salzedella sub-basin
- (X1) Oyster shells, Xert Formation, Forest road Xert-Turmell, Salzedella sub-basin
- (F1) Rudist shells, Forcall Formation, Las Cubetas section, Galve sub-basin**
- (V1) Rudist shells, Villarroya de los Pinares Formation, La Serna Creek, Galve sub-basin**
- (V2) Rudist shells, Villarroya de los Pinares Formation, La Serna Creek, Galve sub-basin**
- (V3) Rudist shells, Villarroya de los Pinares Formation, Las Mingachas, Galve sub-basin**
- (B1) Rudist shells, Benassal Formation, Mola d'en Camaràs, Morella sub-basin
- (B2) Rudist shells, Benassal Formation, Las Corralizas Creek, Galve sub-basin**

*Sequence stratigraphy of European basins (Hardenbol et al.1998, Gradstein et al. 2004)

**Pascual-Cebrian (2014)

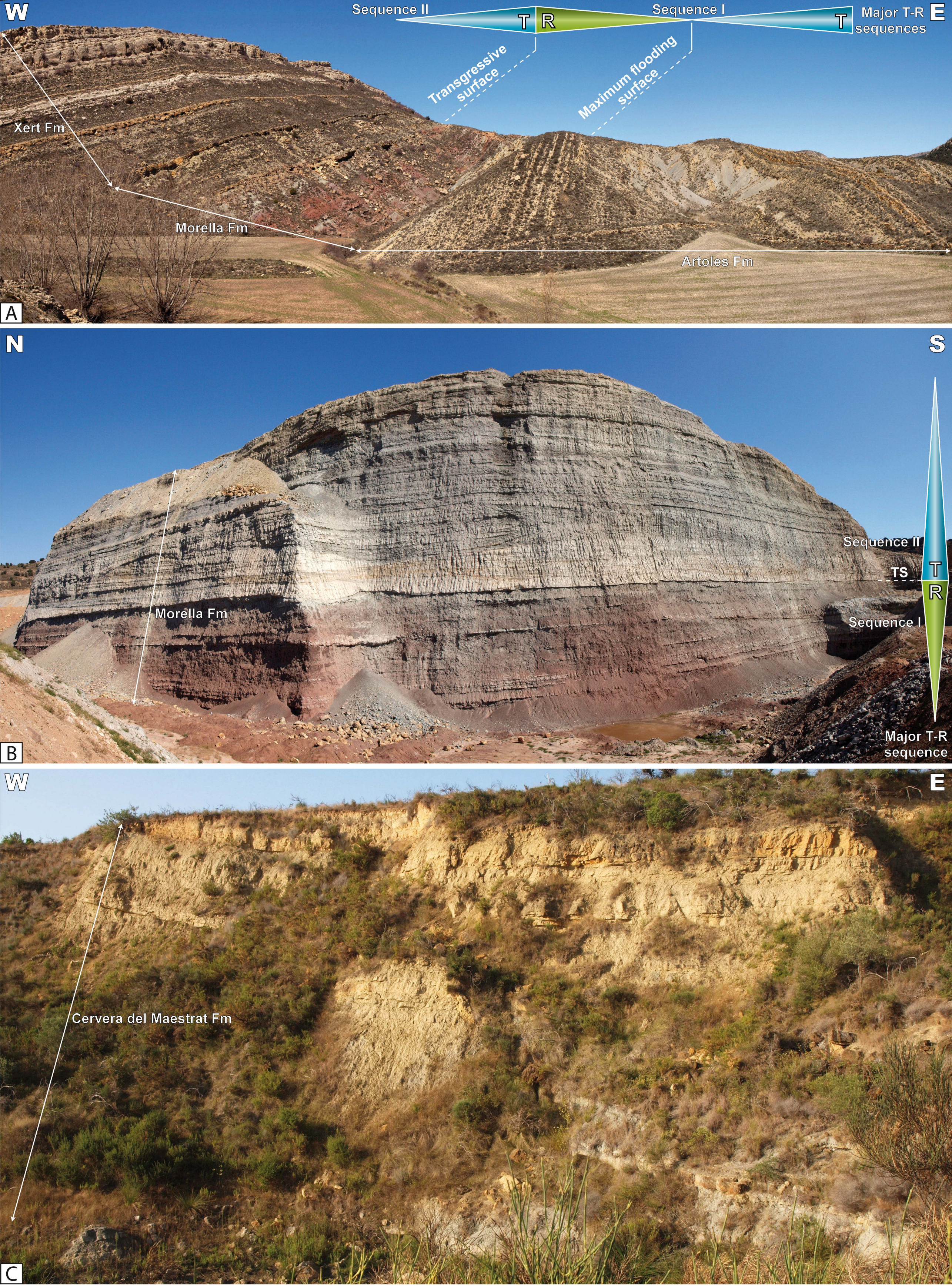

W
Sequence II
T
R
Sequence I
T
E
Major T-R sequences
Transgressive surface
Maximum flooding surface
Xert Fm
Morella Fm
Artoles Fm
A
N
S
Sequence II
TS
T
R
Sequence I
Morella Fm
Major T-R sequence
B
W
E
Cervera del Maestrat Fm
C

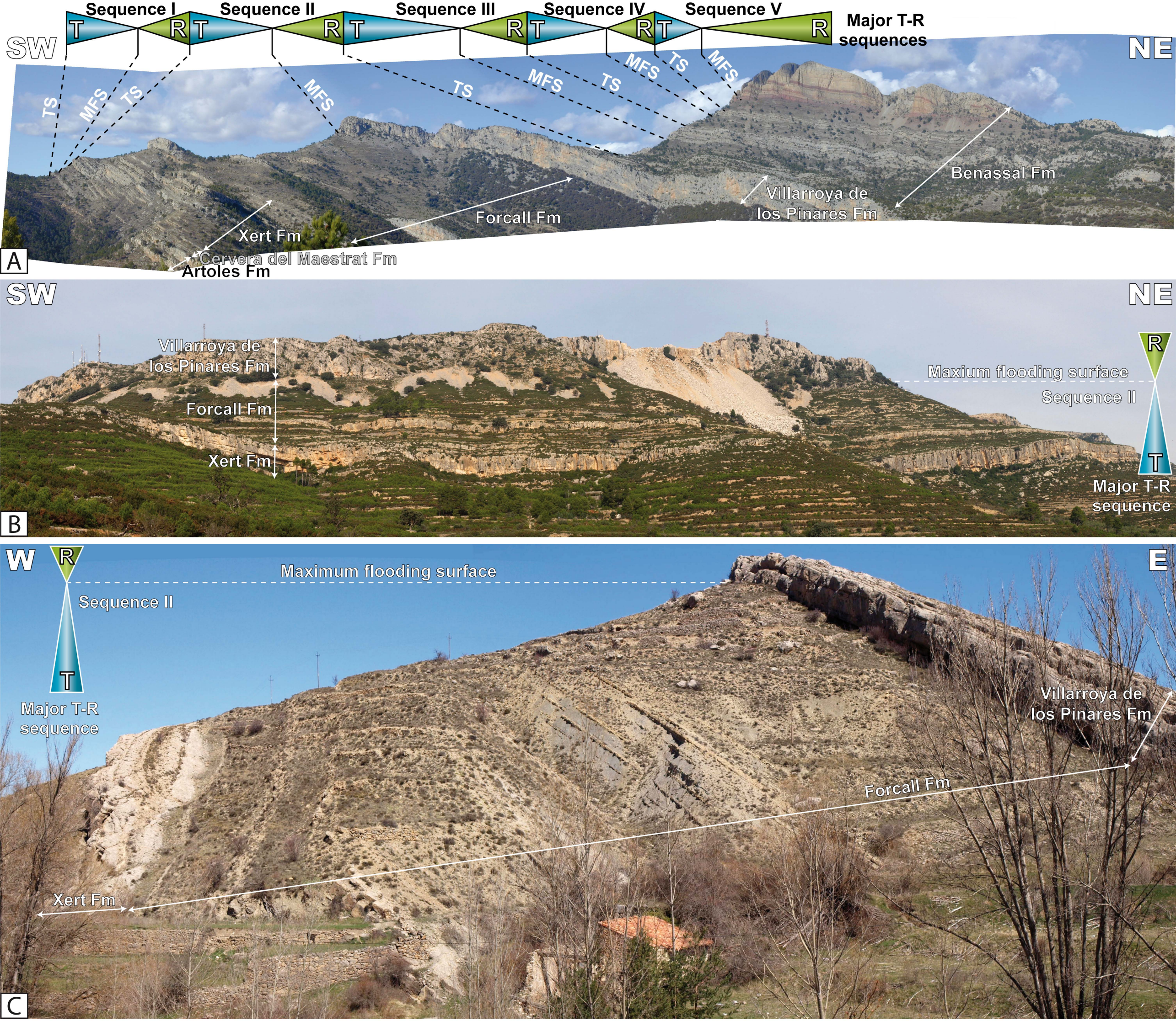

Sequence I
Sequence II
Sequence III
Sequence IV
Sequence V
Major T-R sequences
SW
NE
TS
MFS
Benassal Fm
Villarroya de los Pinares Fm
Forcall Fm
Xert Fm
Cervera del Maestrat Fm
Artoles Fm
A
Maxium flooding surface
Sequence II
Major T-R sequence
B
W
E
Maximum flooding surface
C


E
W
Major T-R sequences
T
Sequence II
R
T
Sequence III
R
MFS
MFS
TS
Benassal Fm
Villarroya de los Pinares Fm
Forcall Fm
Xert Fm
A
SW
NE
Forcall Fm
B
W
E
BenassalFm
Villarroya de los Pinares Fm
Forcall Fm
R
MFS
T
TS
R
MFS
Sequence III
Sequence II
T
Major T-R sequences
C
NW
SE
Major T-R sequence
R
MFS
Sequence III
T
Benassal Fm
D

S
N
Benassal Fm
A
Sequence III
Sequence IV
Sequence V
T
R
T
R
T
R
Major T-R sequences
W
E
MFS
TS
MFS
TS
MFS
Benassal Fm
Forcall Fm
B
SE
NW
Escucha Fm
C

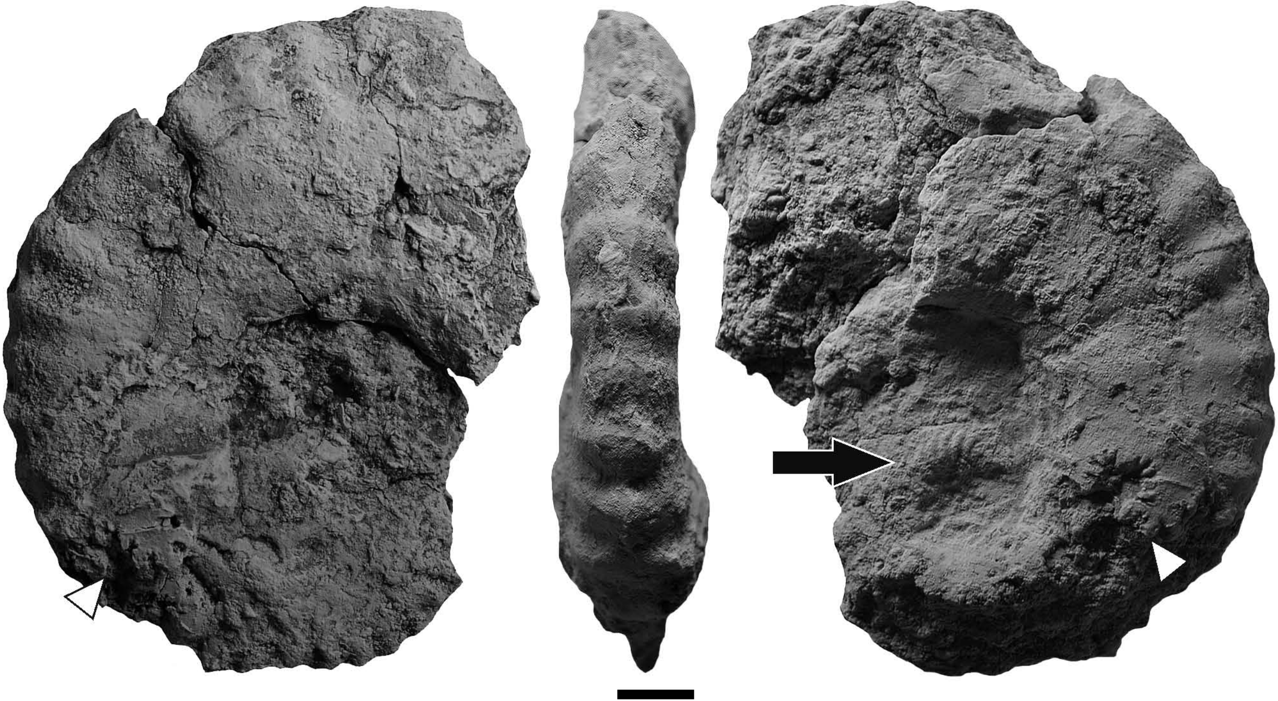

Sample	Locality	Component	Lithostrat. Unit	Mg ppm	Sr ppm	Fe ppm	Mn ppm	$^{87}Sr/^{86}Sr$ measured	2 s.e. (*10^{-6})	$^{87}Sr/^{86}Sr$ corrected	mean	2 s.e. (*10^{-6})	Deg. Alt.	min	Age (Ma)	max
A)																
B1-A	Mola d'en Camaràs	Rudist	Benassal Fm	1172	864	42	1,1	0.707309	0.000007	**0.707315**			P			
B1-B	Mola d'en Camaràs	Rudist	Benassal Fm	521	641	69	10,6	0.707305	0.000007	**0.70731**			PA			
B1-C	Mola d'en Camaràs	Rudist	Benassal Fm	na	na	na	na	0.707301	0.000007	**0.707306**			P			
mean											**0.707310**	0.000007		118.23	**118.93**	119.66
B1-M	Mola d'en Camaràs	matrix	Benassal Fm	3736	228	1335	54.5	0.707466	0.000006	0.707466						
X1-A	Forest road Xert-Turmell	Oyster	Xert Fm	1736	897	116	14.6	0.707433	0.000007	**0.707425**			P			
X1-B	Forest road Xert-Turmell	Oyster	Xert Fm	917	708	291	215,0	0.707432	0.000006	*0.707438*			A			
mean											**0.707425**	0.000013		124.3	**124.94**	125.53
X1-M	Forest road Xert-Turmell	matrix	Xert Fm	4085	452	1948	91.5	0.707546	0.000007	0.707538						
C1-A	Mas del Regall	Oyster	Cervera Fm	813	1310	216	104,0	0.707573	0.000007	*0.707565*			PA			
C1-B	Mas del Regall	Oyster	Cervera Fm	726	1143	337	212,0	0.707521	0.000001	*0.707513*			PA			
C1-C	Mas del Regall	Oyster	Cervera Fm	595	937	296	171,0	0.707474	0.000007	**0.707466**			PA			
mean											**0.707466**	0.000013		125.62	**126.24**	127.01
C1-M	Mas del Regall	matrix	Cervera Fm	2928	295	7812	492,0	0.707941	0.000006	0.707933			PA			
A1-A	Corral d'en Parra	Brachiopod	Artoles Fm	1644	1048	77	8.8	0.70749	0.000007	**0.70749**			P			
A1-B	Corral d'en Parra	Brachiopod	Artoles Fm	3176	1019	188	23.4	0.707479	0.000006	**0.707479**			P			
A2-A	Corral d'en Parra	Oyster	Artoles Fm	888	697	194	21.5	0.707511	0.000007	*0.707511*			PA			
A2-B	Corral d'en Parra	Oyster	Artoles Fm	1034	786	126	25.7	0.707494	0.000006	**0.707494**			P			
mean											**0.707488**	0.000009		126.61	**127.49-128.33**	129.77
A1-M	Corral d'en Parra	matrix	Artoles Fm	2847	462	1085	100,0	0.707613	0.000006	0.707613						
A3-A	Mas del Regall	Oyster	Artoles Fm	473	952	280	82.6	0.707494	0.000007	*0.7075*			PA			
A3-B	Mas del Regall	Oyster	Artoles Fm	884	1112	164	23.8	0.707491	0.000006	**0.707491**			P			
A3-C	Mas del Regall	Oyster	Artoles Fm	1652	791	161	25.6	0.707493	0.000006	**0.707485**			P			
mean											**0.707488**	0.000009		126.61	**127.49-128.33**	129.77
A3-M	Mas del Regall	matrix	Artoles Fm	4378	1371	2753	264,0	0.707554	0.000007	0.707546						
B)																
B2	Barranco de las Corralizas	Rudist	Benassal Fm	1616	1053	362	11.3	0.70729	0.000009	**0.707303**			PA	117.670	**118.47**	119.30
V3	Las Mingachas	Rudist	Villarroya de los Pinares Fm	791	987	681	5.09	0.707343	0.00001	**0.707356**			P	121.28	**122.03**	122.69
V2	Barranco de la Serna	Rudist	Villarroya de los Pinares Fm	1423	1095	250	3.05	0.70734	0.000008	**0.707353**			P	121.22	**121.87**	122.44
V1	Barranco de la Serna	Rudist	Villarroya de los Pinares Fm	1075	1107	135	1.03	0.707348	0.000008	**0.707361**			P	121.68	**122.28**	122.83
F1	Las Cubetas	Rudist	Forcall Fm	1406	894	362	19.01	0.707377	0.00001	**0.707390**			P	123.03	**123.60**	124.13